NMR and NQR fluctuation effects in layered superconductors

D. Fay,[1] J. Appel,[1] C. Timm,[2] and A. Zabel[1]
[1]*I. Institut für Theoretische Physik, Universität Hamburg, Jungiusstr. 9, D-20355 Hamburg, Germany*
[2]*Institut für Theoretische Physik, Freie Universität Berlin, Arnimallee 14, D-14195 Berlin, Germany*
(Received 17 July 2000; published 22 January 2001)

We study the effect of thermal fluctuations of the *s*-wave order parameter of a quasi-two-dimensional superconductor on the nuclear spin relaxation rate near the transition temperature T_C. We consider both the effects of the amplitude fluctuations and the Berezinskii-Kosterlitz-Thouless (BKT) phase fluctuations in weakly coupled layered superconductors. In the treatment of the amplitude fluctuations we employ the Gaussian approximation and evaluate the longitudinal relaxation rate T_1^{-1} for a clean *s*-wave superconductor, with and without pair breaking effects, using the static pair fluctuation propagator $\mathcal{D}$. The increase in T_1^{-1} due to pair breaking in $\mathcal{D}$ is overcompensated by the decrease arising from the single-particle Green's functions. The result is a strong effect on T_1^{-1} for even a small amount of pair breaking. The phase fluctuations are described in terms of dynamical BKT excitations in the form of pancake vortex-antivortex (VA) pairs. We calculate the effect of the magnetic field fluctuations caused by the translational motion of VA excitations on T_1^{-1} and on the transverse relaxation rate T_2^{-1} on both sides of the BKT transition temperature $T_{\mathrm{BKT}}<T_C$. The results for the NQR relaxation rates depend strongly on the diffusion constant D that governs the motion of free and bound vortices as well as the annihilation of VA pairs. We discuss the relaxation rates for real multilayer systems where D can be small and thus increase the lifetime of a VA pair, leading to an enhancement of the rates. We also discuss in some detail the experimental feasibility of observing the effects of amplitude fluctuations in layered *s*-wave superconductors such as the dichalcogenides and the effects of phase fluctuations in *s*- or *d*-wave superconductors such as the layered cuprates.

DOI: 10.1103/PhysRevB.63.064509 PACS number(s): 74.72.−h, 74.25.Nf, 74.40.+k, 74.60.Ge

I. INTRODUCTION

The most common NMR and NQR experiments on high-T_C and other quasi-two-dimensional (quasi-2D) superconductors concern the Knight shift and the longitudinal and transverse relaxation rates. Both of these experiments explore the low-frequency spin dynamics of electrons and holes in normal metals and superconductors. The relaxation rates are caused by the time dependence of the fluctuating magnetic fields. In superconductors these field fluctuations originate from electronic quasiparticle excitations and from the motion of magnetic vortices. In the high-T_C cuprates the quadrupolar Cu spin-lattice relaxation can be due to the transitions between quadrupolar states of the Cu nuclei caused by the interaction of the nuclear spins with the time-dependent magnetic fields of the vortices. The 2D cuprates such as Bi-2212 consist of CuO_2 layers with a very small interlayer hopping matrix elememt $t_\perp$.[1] The magnetic field fluctuations near the real superconducting transition temperature T_C, where the resistivity goes to zero and the long-range order is established by Josephson phase coupling, are caused by both the quasiparticle excitations of the normal and superconducting states and by the spontaneous excitation of thermal vortex-antivortex (VA) pairs. These vortex excitations occur close to the Berezinskii-Kosterlitz-Thouless (BKT) transition temperature of a 2D layer, $T_{\mathrm{BKT}}<T_C$; cf. Fig. 1.[2–4] Whereas the long-wavelength Gaussian fluctuations of the quasiparticle excitations consist of amplitude and long-wavelength phase fluctuations of the complex order parameter, the VA fluctuations are primarily phase fluctuations of the order parameter. The BKT scenario also applies to 2D layers that are weakly coupled by electromagnetic and Josephson coupling effects.[5–7] Around the real transition temperature T_C there exists the narrow Ginzburg regime of critical fluctuations where the Josephson and Coulomb couplings into the third dimension begin to establish the phase coherence between neighboring layers. This is represented by the shaded area around T_C in Fig. 1. According to the detailed calculations of the specific heat fluctuations of Ramallo and Vidal[8] and their comparison with experimental results, the three-dimensional critical behavior is restricted to a rather narrow range in the cuprates, $t\equiv|T-T_C|<10^{-2}$, so that a wide region of Gaussian fluctuations of the order of 10 K exists above T_C. The same considerations should be be valid for the dichalcogenides which are layered systems exhibiting *s*-wave pairing. The BKT vortex-antivortex fluctuations exist above T_C below the mean-field transition temperature T_{C0} (cf. Fig. 1). At $T_{cr}>T_C$, the interlayer phase coherence becomes so weak that the Josephson vortices proliferate and the 3D phase coupling ceases to exist.

In Sec. II we study the effect of Gaussian fluctuations on

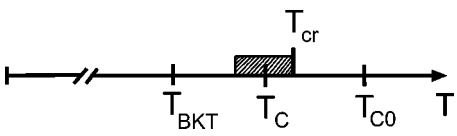

FIG. 1. Temperature regions. The mean-field transition temperature of a 2D layer is given by T_{C0}. The regime of long-wavelength Gaussian fluctuations with 2D character lies outside the shaded region of strong 3D fluctuations. Vortex-antivortex fluctuations exist above T_{BKT} in a single layer. In a 3D system of weakly coupled layers, coming from high temperatures, the 2D fluctuations are cut off at the crossover temperature T_{cr}, before the true transition temperature T_C is reached.

the spin-lattice relaxation rate of *s*-wave superconductors near the transition temperature for layered systems. The NMR spin relaxation rate T_1^{-1} has been investigated intensively in the high-T_C superconductors. At present, however, the general opinion seems to be that only the electron-doped high-T_C superconductors may exhibit *s*-wave pairing.[9,10] Other layered compounds with *s*-wave pairing are the layered transition metal dichalcogenides. Long-wavelength thermal fluctuations of the superconducting order parameter, i.e., Gaussian fluctuations, are expected to play a pertinent role in layered compounds for several reasons—in particular, the quasi-2D structure of these metallic systems, the small coherence length ξ_0 in the layers (cuprates), and the large penetration depth λ for fields parallel to the layers. The effect of such fluctuations on T_1^{-1} in these and similar systems has been the subject of numerous papers.[11–21] Most of the previous authors[13,14,17–19,21] included nonmagnetic impurity scattering and also set the small external NMR frequency ω equal to zero. In such theories it is not clear whether the correct clean limit is obtained. For example, in a clean system without pair breaking, we find $1/T_1 \propto 1/\omega$, for $T \to T_C$. To elucidate this limit we consider a clean system from the outset. This may be a reasonable first approximation for systems like the cuprates where ξ_0 is large compared with the mean free path *l*.

Certainly for the cuprates, and many other layered systems as well, it is important to include the pair breaking effect of inelastic scattering due to the exchange of low-energy bosons, spin fluctuations, or phonons, for example. To do this correctly would require solution of the strong-coupling Eliashberg equations, taking full account of the energy dependence of the pairing interaction and the single-particle self-energy. To date no such theory has appeared in the literature with respect to NMR in layered systems for *s*-wave pairing.[22] In previous weak-coupling theories inelastic scattering has usually been accounted for by introducing a cutoff in the pair fluctuation propagator or a constant lifetime in the single-particle Green's function. We also do a weak-coupling calculation and simulate the effect of inelastic scattering through a pair breaking parameter in analogy to magnetic impurity scattering. The large qualitative and quantitative effect of pair breaking indicates that the results of a weak-coupling calculation should be viewed with caution until they can be confirmed with a strong coupling Eliashberg calculation. Since the inclusion of pair breaking in the clean case qualitatively changes the results, we give some of the details both with and without pair breaking.

In Sec. III we study the effect of topological intralayer phase fluctuations (vortices) on the NQR spin-lattice and spin-spin relaxation rates T_1^{-1} and T_2^{-1}. In contrast to the Gaussian fluctuations of Sec. II, which contain the long-wavelength fluctuations of the amplitude of the order parameter, the topological fluctuations are, primarily, the 2D singular phase fluctuations of the superconducting order parameter. Experimentally, the relaxation rates $T_{1,2}^{-1}$ in the cuprates can be obtained in zero magnetic field from NQR spin-echo experiments on ^{63}Cu and ^{65}Cu nuclei. We consider NQR to allow direct application of the zero-field BKT theory. The translational motion of vortices and antivortices and the corresponding time-dependent magnetic fields not only affect the nuclear spin relaxation but also the NQR linewidth and for this reason we calculate, in addition to T_1^{-1}, the spin-phase relaxation rate T_2^{-1}. The distribution of VA pairs is determined by the singular parts of the otherwise smooth phase fields of the complex order parameter. The topological VA excitations reduce the transition temperature of a single layer to the Berezinskii-Kosterlitz-Thouless temperature T_{BKT}, above which the bound VA pairs begin to break up into free pancake vortices and antivortices. We study, in the temperature regime above T_{BKT}, the magnetic field correlation functions that determine T_1^{-1} and T_2^{-1}. The magnetic field fluctuations are caused by the translational motion of the thermally excited vortices and antivortices. The diffusion constant of the vortices and antivortices, $D(T)$, plays a crucial role for the magnitudes of the relaxation rates; it determines both the free vortex and antivortex motions and the recombination time of a VA pair. We find that D must be sufficiently small in order to get vortex relaxation rates $T_{1,2}^{-1}$ that are comparable to those caused by quasiparticle relaxation. The latter cause relaxation rates of the order of 10^2–$10^3\ \mathrm{s}^{-1}$ near T_C of the cuprates. The effect of the time-varying magnetic fields due to the VA fluctuations on T_2^{-1} is also of some interest for the following reason: Of the two mechanisms causing the transverse relaxation in the cuprates—namely, the indirect nuclear spin-spin coupling and the spin-lattice relaxation—we expect that only the second contribution is affected by the VA fluctuations. These fluctuations lead to an exponential decay of the time-dependent transverse magnetization of the ^{63}Cu or ^{65}Cu nuclear spins.[23] On the other hand, the individual ^{63}Cu-^{63}Cu indirect coupling leads to a Gaussian time decay and is of such short range, $r \ll \xi_0$,[24] that this coupling remains altogether unaffected by the transition into the superconducting state.

In Sec. IV we discuss the experimental situation in some detail with respect to the possibility of observing the effect of superconducting fluctuations on the longitudinal and transverse relaxation rates of the nuclear spins in layered systems such as the cuprates with *s*-wave pairing and conventional layered superconductors such as the transition metal dichalcogenides.

II. EFFECT OF PAIRING FLUCTUATIONS ON T_1^{-1}

A. General formalism

The NMR spin relaxation rate is given by

$$\frac{1}{T_1 T} = \sum_{\mathbf{q}} A_{\mathbf{q}} \frac{\mathrm{Im}\,\chi(\mathbf{q},\omega)}{\omega}, \tag{1}$$

where χ is the transverse (spin-flip) susceptibility, ω is the external frequency, and $A_{\mathbf{q}}$ is determined by the fine structure constants and should be large for the $\mathbf{q}$'s that couple to large values of $\mathrm{Im}\,\chi(\mathbf{q},\omega)$. Here we assume that $A_{\mathbf{q}}$ is a constant. The susceptibility diagrams through first order in the Cooper pair fluctuation propagator, $\mathcal{D}$, are shown in Fig.

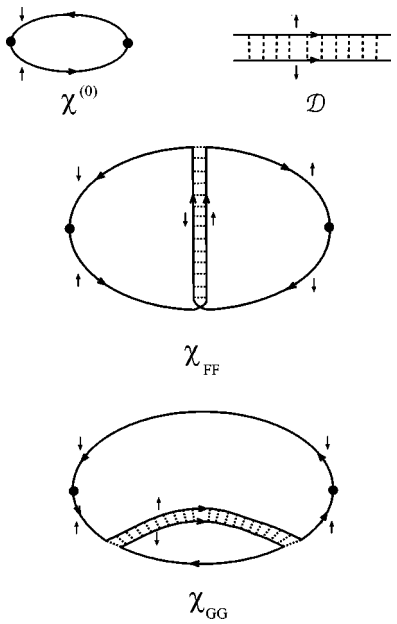

FIG. 2. Transverse susceptibility diagrams through first order in the pair fluctuation propagator $\mathcal{D}$.

2. The zeroth-order contribution $\chi^{(0)}$ yields Korringa's law in the normal phase and, in the absence of pair breaking, the Hebel-Slichter peak below T_C for *s*-wave pairing. The leading fluctuation contributions are given by the diagrams χ_{FF} and χ_{GG}. We follow the notation of Maniv and Alexander,[12] who considered the clean case in 3D, and write

$$\sum_{\mathbf{q}} \mathrm{Im}\,\chi(\mathbf{q},\omega) = \mathrm{Im}\,\chi(\omega), \tag{2}$$

where

$$\mathrm{Im}\,\chi(\omega) = \mathrm{Im}\,\chi_{FF}(\omega) + \mathrm{Im}\,\chi_{GG}(\omega). \tag{3}$$

The first term represents the Maki-Thompson (MT) diagram,[25,26] $\chi_{FF} = \chi_{MT}$, which also has a long history in the calculation of the fluctuation conductivity. The second term accounts for the self-energy or density of states (DOS) effect that is caused by the renormalization of the normal-state Green's functions by superconducting fluctuations. This contribution is often denoted by $\chi_{DOS} = \chi_{GG}$.[17–19,21] The second-order (Aslamazov-Larkin) diagram does not contribute to transverse susceptibility.

We define the static fluctuation propagator $\mathcal{D}$ in terms of the particle-particle *t* matrix as

$$\mathcal{D}(\mathbf{k}) = -k_B T t(\mathbf{k},0), \tag{4}$$

where

$$t^{-1}(\mathbf{k}, i\nu_m) = V^{-1} - k_B T \sum_{i\omega_n} \frac{d^3k'}{(2\pi)^3} G(\mathbf{k}', i\omega_n) \times G(\mathbf{k}-\mathbf{k}', i\nu_m - i\omega_n)\,\gamma. \tag{5}$$

Here $\omega_n = \omega_n(T) = (2n+1)\pi k_B T$, k is the total momentum of the Cooper pair, γ is the impurity vertex, and we have taken the pair interaction V to be constant. $\mathcal{D}(k)$ diverges when T approaches T_C from above for k equal to zero, signaling the transition to the superconducting phase and defining T_C. In order to describe static Gaussian fluctuations, the *t* matrix is calculated for small total momentum with zero-order Green's functions. A standard weak-coupling calculation[27] yields for a clean system ($\gamma = 1$)

$$\mathcal{D}^{-1}(k) = \left(\frac{N_0\pi}{k_B T}\right)\left\{ \sum_{\omega_n(T_C)} \frac{k_B T_C}{|\omega_n(T_C)|} - \sum_{\omega_n(T)} \frac{k_B T}{|\omega_n(T)|} + \frac{(\hbar v_F k)^2}{12} \sum_{\omega_n(T)} \frac{k_B T}{|\omega_n(T)|^3} \right\}, \tag{6}$$

where $N_0 = ma^2/(2\pi\hbar^2)$ is the 2D density of states per spin and v_F is the Fermi velocity. All the sums are cut off at the constant BCS cutoff ω_C. The cutoff on n, $n_c = \omega_c/2\pi T - \frac{1}{2}$, depends on T and is responsible for the important difference in the first two sums in Eq. (6).[28] Performing the sums leads to

$$\mathcal{D}(k) = \frac{k_B T/N_0}{\ln(T/T_C) + \xi^2 k^2}, \tag{7}$$

where ξ is related to the BCS coherence length $\xi_0 = \xi(T=0)$,

$$\xi = \sqrt{\frac{7\zeta(3)}{48}} \frac{\hbar v_F}{\pi k_B T} = \xi_0 T_C/T. \tag{8}$$

In the early conductivity calculations it was first observed that the Maki diagram has anomalous properties: In the presence of nonmagnetic impurity scattering, the impurity vertex corrections at each end of the fluctuation propagator $\mathcal{D}$ in the polarization bubble lead to a divergence at all temperatures in 2D. This divergence could be removed by including a pair breaking parameter.[26,29] We emphasize that we work in the clean limit where there is no impurity vertex in the first place and thus this ''Maki divergence'' does not occur. As we will see, however, this contribution is also rather pathological in a clean system in 2D: We find that it diverges at all temperatures when ω goes to zero. This divergence is removed (except right at $T = T_C$) by the inclusion of pair breaking.

The Maki-Thompson contribution to T_1^{-1}, χ_{FF}, was first evaluated in 2D by Kuboki and Fukuyama[13] in the dirty limit for $\omega = 0$. They found a logarithmic divergence on approaching T_C from above with the form $\ln(\Gamma/t)$ where Γ is a pair breaking parameter. This presented a problem in the high-T_C superconductors because no corresponding peak has been observed there. An attempt to remedy this situation was made by Heym[14] who generalized Kuboki and Fukuyama's work by including the frequency dependence of $\mathcal{D}$. He found that dynamic fluctuations become important for $T/T_C \geqslant 1.05$ and can lead to a significant correction to the T dependence of $1/T_1$ for these temperatures, in particular for strong pair breaking. The large peak for $T \to T_C$ remains, however. We will see later that pair breaking can strongly reduce this peak.

We follow the notation of Maniv and Alexander[12] and write in 2D

$$\chi_{FF}(i\Omega_\nu)=\sum_{\mathbf{k}} C(\mathbf{k},i\Omega_\nu)\mathcal{D}(k), \tag{9}$$

$$\chi_{GG}(i\Omega_\nu)=\sum_{\mathbf{k}} A(\mathbf{k},i\Omega_\nu)\mathcal{D}(k), \tag{10}$$

where the contributions of the polarization diagrams are given by

$$C(\mathbf{k},i\Omega_\nu)=-k_BT\sum_n \sum_{\mathbf{p}_1,\mathbf{p}_2} G(\mathbf{p}_1,i\omega_n)G(\mathbf{k}-\mathbf{p}_1,-i\omega_n) \times G(\mathbf{p}_2,i\omega_n+i\Omega_\nu)G(\mathbf{k}-\mathbf{p}_2,-i\omega_n-i\Omega_\nu) \tag{11}$$

and

$$A(\mathbf{k},i\Omega_\nu)=2k_BT\sum_n \sum_{\mathbf{p}_1,\mathbf{p}_2} G^2(\mathbf{p}_1,i\omega_n) \times G(\mathbf{k}-\mathbf{p}_1,-i\omega_n)G(\mathbf{p}_2,i\omega_n+i\Omega_\nu). \tag{12}$$

The G's are taken to be zero-order propagators of the form (for the case of no pair breaking) $G(\mathbf{p},i\omega_n)=(i\omega_n-\xi_\mathbf{p})^{-1}$ where we assume free particles in 2D, $\xi_\mathbf{p}=p^2/2m-E_F$. Since $\mathcal{D}(k)$ is peaked at small k, we approxoimate $\xi_{\mathbf{k}-\mathbf{p}} \approx \xi_\mathbf{p}-v_Fk\cos\phi$ where $\phi=\angle(\mathbf{k},\mathbf{p})$. The factor of 2 in Eq. (12) accounts for the two diagrams of the GG type.

B. Clean system without pair breaking

We consider first the Maki-Thompson diagram. Performing the integrals over $\xi_{\mathbf{p}_1}$ and $\xi_{\mathbf{p}_2}$ in Eq. (11) we have

$$C(\mathbf{k},i\Omega_\nu)=N_0^2\pi^2T\sum_n \mathrm{sgn}(\omega_n)\mathrm{sgn}(\omega_n+\Omega_\nu)\int_0^{2\pi}\frac{d\phi_1}{2\pi} \times\int_0^{2\pi}\frac{d\phi_2}{2\pi}\frac{1}{(i\omega_n-v_1k/2)(i\omega_n+i\Omega_\nu-v_2k/2)}. \tag{13}$$

Due to the sgn functions, it is mathematically convenient to follow Maniv and Alexander[12] and split the contribution into two parts:

$$\mathrm{Im}\,\chi_{FF}(\omega)=\mathrm{Im}\,\chi_{FF}^{(1)}(\omega)+\mathrm{Im}\,\chi_{FF}^{(2)}(\omega), \tag{14}$$

where

$$\mathrm{Im}\,\chi_{FF}^{(j)}(i\Omega_\nu)=N_0^2\sum_{\mathbf{k}}\mathcal{D}(k)\int_0^{2\pi}\frac{d\phi_1}{2\pi} \times\int_0^{2\pi}\frac{d\phi_2}{2\pi}\Pi_j(\varepsilon_1,\varepsilon_2,i\Omega_\nu), \tag{15}$$

with $\varepsilon_i=kv_F\cos\phi_i/2$, $j=1,2$, and

$$\Pi_1(\varepsilon_1,\varepsilon_2,i\Omega_\nu)=\pi^2k_BT\sum_{n=-\infty}^{+\infty}\frac{1}{(i\omega_n-\varepsilon_1)(i\omega_n-\varepsilon_2+i\Omega_\nu)}, \tag{16}$$

$$\Pi_2(\varepsilon_1,\varepsilon_2,i\Omega_\nu)=-2\pi^2k_BT\begin{cases}\displaystyle\sum_{n=-\nu}^{-1}\frac{1}{(i\omega_n-\varepsilon_1)(i\omega_n-\varepsilon_2+i\Omega_\nu)}, & \nu>0,\\ \displaystyle\sum_{n=0}^{|\nu|-1}\frac{1}{(i\omega_n-\varepsilon_1)(i\omega_n-\varepsilon_2+i\Omega_\nu)}, & \nu<0.\end{cases} \tag{17}$$

For a clean system this decomposition is done merely for mathematical convenience.[12] When impurity scattering is present, however, the singular q dependence due to the impurity vertices at the ends of the $\mathcal{D}$ propagator (the ''Maki divergence,'' again) makes it necessary to split χ_{FF} in a different manner into a ''regular'' and an ''anomalous'' part.[17] Performing the sum over n in Eq. (16) and analytically continuing $i\Omega_\nu$ to the real external frequency ω, we find, to leading order in ω,

$$\mathrm{Im}\,\chi_{FF}^{(1)}(\omega)=\left[\left(\frac{a}{\xi_0}\right)^2\frac{\hbar\omega}{E_F}\frac{N_0}{2}\right]\int_{\underline{\Omega}}^{\Lambda}\mathcal{D}(x)dx \times\int_{-1}^{1-2\overline{\Omega}/x}\frac{dy}{\sqrt{1-y^2}}\frac{(-1)f'(\varepsilon_cxy/\overline{T})}{\sqrt{1-(2\overline{\Omega}/x+y)^2}}, \tag{18}$$

$$\mathcal{D}(x)=\frac{N_0\zeta^2}{k_BT}\mathcal{D}(k)=\frac{\overline{T}^2}{x^2+t(\overline{T}/\zeta)^2}, \tag{19}$$

where we have defined $x=k/k_F$, $\bar{\Omega}=\hbar\omega/2E_F$, $\varepsilon_c=E_F/k_BT_C$, $\bar{T}=T/T_C$, $\zeta=k_F\xi_0$, and $t=\ln\bar{T}\approx(T-T_C)/T_C$. Here f' is the derivative of the Fermi function and Λ is a cutoff which we take as $O(1)$. A larger cutoff does not change the results significantly. Note that, since $-f'$ is positive, $\mathrm{Im}\,\chi^{(1)}_{FF}$ is a positive contribution, proportional to N_0^2.

After analytic continuation and expansion to first order in ω we find from Eqs. (15) and (17)

$$\mathrm{Im}\,\chi^{(2)}_{FF}(\omega)=\left[\left(\frac{a}{\xi_0}\right)^2\frac{\hbar\omega}{E_F}\frac{N_0}{2}\right]\left[\frac{\varepsilon_c}{\pi\bar{T}}\right]\int_0^\Lambda x\mathcal{D}(x)dx \times\int_0^{2\pi}d\phi_1\int_0^{2\pi}d\phi_2 \times\sum_{n=0}^{\infty}\left\{\frac{p_n\mu_1^2\mu_2^2-p_n^5}{(p_n^2+\mu_1^2)^2(p_n^2+\mu_2^2)^2}\right\}, \tag{20}$$

where $\mu_i=\varepsilon_c x\cos\phi_i/\bar{T}$, $p_n=(2n+1)\pi$, and several terms that vanish after the angular integrations have been omitted. $\mathrm{Im}\chi^{(2)}_{FF}$ is negative.

We turn now to the calculation of the DOS contribution χ_{GG} and first evaluate the sum over n in Eq. (12) as a contour integration and then carry out the analytic continuation $i\Omega_{nu}\to\omega+i\delta$. Of the several resulting terms only the following yields, after the angular integrations, a nonvanishing contribution to first order in ω:

$$A(\mathbf{k},\omega)=4\pi N_0\sum_{\mathbf{p}_1}\times\int_{-\infty}^{+\infty}\frac{-f(\xi_2)d\xi_2}{(\xi_2-\xi_1-\omega-i\delta)^2(\xi_2+\xi_1-\mathbf{v}\cdot\mathbf{k}-\omega-i\delta)}. \tag{21}$$

The ξ_2 integral can be expressed as a sum of the residues at the poles of the Fermi function:

$$A(\mathbf{k},\omega)=8\pi^2 iN_0k_BT\times\sum_{\mathbf{p}_1}\sum_{n=-1}^{-\infty}\frac{1}{(i\omega_n-\xi_1-\omega)^2(\imath\omega_n+\xi_1-\mathbf{v}\cdot\mathbf{k}-\omega)}. \tag{22}$$

Expanding to first order in ω and performing the ξ_1 integration we obtain the negative contribution

$$\mathrm{Im}\,\chi_{GG}(\omega)=-\left[\left(\frac{a}{\xi_0}\right)^2\frac{\hbar\omega}{E_F}\frac{N_0}{2}\right]\left[\frac{8\varepsilon_c}{\pi\bar{T}}\right]\int_0^\Lambda x\mathcal{D}(x)dx\int_0^{\pi/2}d\phi \times\sum_{n=0}^{\infty}\left\{\frac{p_n[p_n^2-3(x\varepsilon_c\cos\phi/\bar{T})^2]}{[p_n^2+(x\varepsilon_c\cos\phi/\bar{T})^2]^3}\right\}. \tag{23}$$

In Fig. 3 we plot the three contributions to $\mathrm{Im}\,\chi$ as functions of the reduced temperature $\bar{T}=T/T_C$. The positive contribution $\mathrm{Im}\,\chi^{(1)}_{FF}$ is seen to dominate strongly.

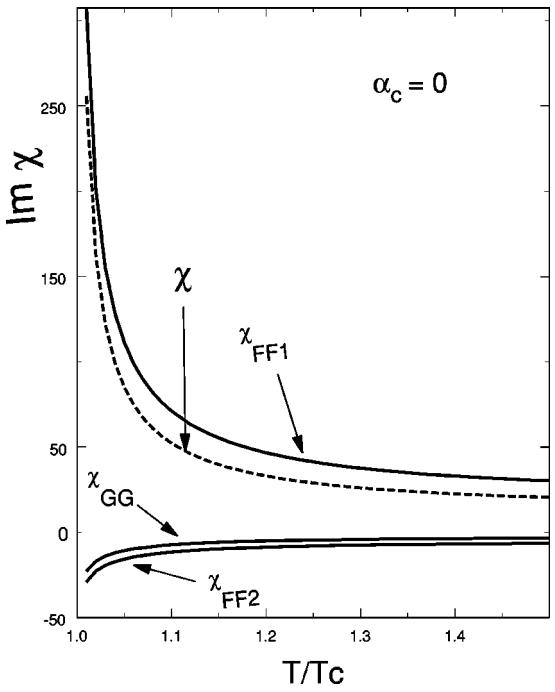

FIG. 3. The three fluctuation contributions to $\mathrm{Im}\,\chi(\omega)=\Sigma_{\mathbf{q}}\,\mathrm{Im}\,\chi(\mathbf{q},\omega)$ for a clean system without pair breaking measured in units of $[(a/\xi_0)^2(\hbar\omega/E_F)N_0/2]$.

It is interesting to consider these results in the limit of $T\to T_C$ from above. The experimental external frequency ω is very small but we leave it finite since $\mathrm{Im}\,\chi_{FF}$ depends on the ratio t/ω. In Eqs. (20) and (23) the function $x\mathcal{D}(x)\propto x/(x^2+t\bar{T}^2/\zeta^2)$ is peaked at small x for t small. The sum over n is only weakly dependent on x for small x and it is a good first approximation to set $x=0$ within the sum. The t dependence then arises solely from the x integration over the fluctuation propagator and one easily finds

$$\frac{\mathrm{Im}\,\chi^{(2)}_{FF}}{\omega}\propto\ln t,\quad \frac{\mathrm{Im}\,\chi_{GG}}{\omega}\propto\ln t,\quad \text{for } t\to 0. \tag{24}$$

These limiting functions are independent of ω. In Eq. (18) for $\mathrm{Im}\,\chi^{(1)}_{FF}$ the limiting behavior is not just due to the fluctuation propagator but is strongly affected by the integral over y. We find the following result:

$$\frac{\mathrm{Im}\,\chi^{(1)}_{FF}}{\omega}\propto\begin{cases}\dfrac{1}{\sqrt{t}}\ln\left(\dfrac{E_F\sqrt{t}}{\omega}\right) & \text{for } \dfrac{\omega}{E_Ft}\to 0,\\[2ex] \dfrac{1}{\omega} & \text{for } \dfrac{E_Ft}{\omega}\to 0.\end{cases} \tag{25}$$

For comparison we give the corresponding results for small t and ω for the clean 3D case:[12]

$$\frac{\mathrm{Im}\,\chi^{(1)}_{FF}}{\omega}\propto\ln\left(\frac{1}{t+c_1\omega^2}\right),\quad \frac{\mathrm{Im}\,\chi^{(2)}_{FF}}{\omega}\propto c_2,\quad \frac{\mathrm{Im}\,\chi_{GG}}{\omega}\propto -c_3, \tag{26}$$

where c_1, c_2, and c_3 are positive constants. In comparison to 3D, the results in 2D are rather pathological. In 3D the only

divergence occurs in $\mathrm{Im}\,\chi_{FF}^{(1)}/\omega$ and then only when *both* t and ω go to zero. In 2D, $\mathrm{Im}\,\chi_{FF}^{(2)}/\omega$ and $\mathrm{Im}\,\chi_{GG}/\omega$ diverge only for $t\to 0$, while $\mathrm{Im}\,\chi_{FF}^{(1)}/\omega$ diverges as $\omega\to 0$ *for all t*. This strange behavior is presumably unphysical and is removed by a small amount of pair breaking. As seen from Eq. (25), the limiting value of $\mathrm{Im}\,\chi_{FF}^{(1)}/\omega$ depends on the ratio ω/t. As $t\to 0$ there is a ''crossover'' near $t=\omega/E_F$ which is probably too close to $t=0$ to be experimentally observable. In any case, for finite ω there is no divergence in $\mathrm{Im}\,\chi_{FF}^{(1)}/\omega$ for $t\to 0$.

It is also interesting to compare our Eq. (25) with the corresponding result of Randeria and Varlamov[17] (RV) who give a result for the ''ultraclean'' limit of a theory that includes elastic scattering from the beginning. Their Eq. (16) reads

$$\mathrm{Im}\,\chi_{FF}\propto\frac{1}{\sqrt{t}}\ln(T_C\tau\sqrt{t})\quad\text{for } T_C\tau\sqrt{t}\gg 1\quad\text{and }\omega=0, \tag{27}$$

where τ is the lifetime for elastic scattering. Since this equation does not contain their pair breaking parameter δ, it should be valid for the case of no pair breaking. Equations (25) and (27) are similar in several respects. In both cases there is a prefactor $1/\sqrt{t}$ multiplied by the logarithm of a large number proportional to $\sqrt{t}$. Since RV set $\omega=0$ before the calculation while we have $1/\tau=0$, an exact comparison of the results is not possible. In the exact clean limit Eq. (25) seems preferable because ω, although very small, is a well-defined experimental quantity while τ in Eq. (27) is not well known and, more importantly, τ should not even appear in the exact result for a clean system. Also, the limit $t\to 0$ is only possible if ω remains nonzero.

C. Clean system with pair breaking

By ''pair breaking'' we mean essentially the effects of inelastic scattering which, in the high-T_C superconductors, for example, could be due to spin fluctuations and phonons. In order to obtain a rough estimate of this effect we want to simulate it in a simple manner within a weak-coupling theory. Our procedure is equivalent to adding a constant inelastic scattering rate to the single-particle propagator as done by other authors.[21] We attempt to justify this physically by assuming that the effect on the fluctuation propagator $\mathcal{D}$ is similar to the well-known pair breaking effect of scattering by magnetic impurities.[28] Impurity scattering affects $\mathcal{D}$ in two ways: self-energy corrections to the single-particle propagators of the t-matrix ladder and vertex corrections to the pair interaction. For nonmagnetic impurities these two contributions cancel for s-wave pairing (Anderson's theorem). For magnetic impurities there is no cancellation and the transition temperature is strongly reduced. For our purposes it is sufficient to retain only the self-energy corrections and to assume that the vertex correction is included in the effective pairing interaction. The Green's functions in Eq. (5) thus have the form

$$G(\mathbf{k},i\omega_n)=\frac{1}{i\tilde{\omega}_n-\xi_{\mathbf{k}}}, \tag{28}$$

with

$$\tilde{\omega}_n=\omega_n+\Gamma\,\mathrm{sgn}(\omega_n), \tag{29}$$

where $\Gamma\equiv\hbar/2\tau_\phi$ is the phenomenological pair breaking parameter destroying the phase coherence between the Cooper pairs. Equation (6) for $\mathcal{D}$ is now replaced by

$$\mathcal{D}^{-1}(k)=\left(\frac{N_0\pi}{k_BT}\right)\left\{\sum_{\omega_n(T_{C0})}\frac{k_BT_{C0}}{|\omega_n(T_{C0})|}-\sum_{\omega_n(T)}\frac{k_BT}{|\tilde{\omega}_n(T)|}+\frac{(\hbar v_Fk)^2}{12}\sum_{\omega_n(T)}\frac{k_BT}{|\tilde{\omega}_n(T)|^3}\right\}, \tag{30}$$

where T_{C0} is the transition temperature in the absence of pair breaking. Although we report here only results for Γ constant, in general Γ will be a function of ω_n. For comparison, for Γ constant the sums can be carried out analytically and Eq. (30) can be expressed in terms of the digamma and tetragamma functions in the notation of Eq. (19) as

$$\mathcal{D}^{-1}(x)=\frac{1}{\zeta^2}\left[\ln\left(\frac{T}{T_{C0}}\right)-\Psi\left(\frac{1}{2}\right)+\Psi\left(\frac{1}{2}+\alpha\right)\right]-\left(\frac{x^2}{14\zeta(3)\overline{T^2}}\right)\Psi^{(2)}\left(\frac{1}{2}+\alpha\right), \tag{31}$$

where

$$\alpha=\frac{\Gamma}{2\pi k_BT}. \tag{32}$$

The transition temperature in the presence of pair breaking, T_C, is obtained by setting $\mathcal{D}(0)^{-1}$ equal to zero, yielding the Abrikosov-Gorkov equation.[30] Since we assume the pair breaking is due to inelastic scattering, T_{C0} is not experimentally accessible. Thinking for the moment of the high-T_C superconductors, in our numerical calculations we take $T_C=100$ K as experimentally given and T_{C0} will be determined by the damping parameter Γ. Although $T_C<T_{C0}$, as expected, $\mathcal{D}$ as a function of k can be modified by the pair breaking in such a way that, neglecting the effect of pair breaking in the rest of the susceptibility diagrams, the fluctuation contributions to T_1^{-1} are increased. To elucidate this behavoir we show $\mathcal{D}$ as a function of $x=k/k_F$ in Fig. 4 for $T=1.03T_C$ and several values of $\alpha_C=\alpha\overline{T}$. The figure shows that the maximum and width of $\mathcal{D}(k)$ increase with Γ. The fact that the fluctuation propagator $\mathcal{D}$ increases with increasing pair breaking may seem counterintuitive if one assumes, in analogy to the case of magnetic impurities where T_{C0} is known, that pair breaking→reduced tendency to superconductivity→weaker fluctuations. In that case, for T fixed relative to T_{C0}, the fluctuations weaken with increasing Γ because T_C and, thus, the divergence of $\mathcal{D}$ are moving away from the reference point T. In our case, however, T is fixed

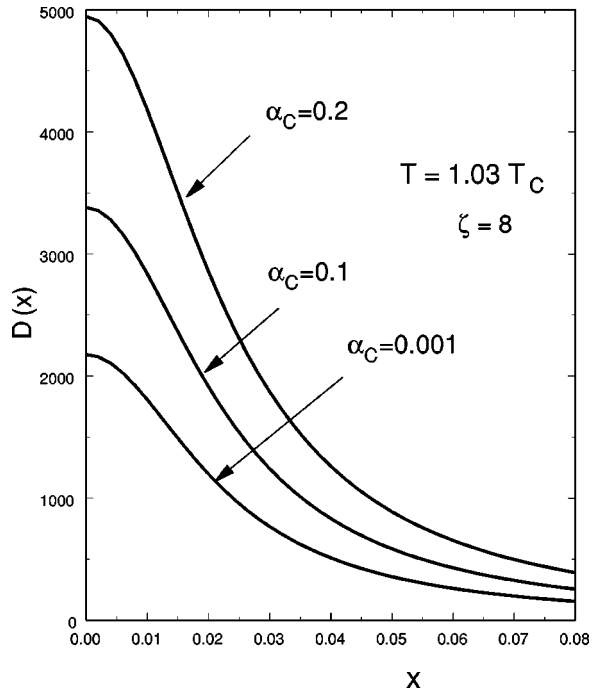

FIG. 4. The fluctuation propagator $\mathcal{D}$ as a function of momentum $x=k/k_F$ for several values of the pair breaking parameter α_C.

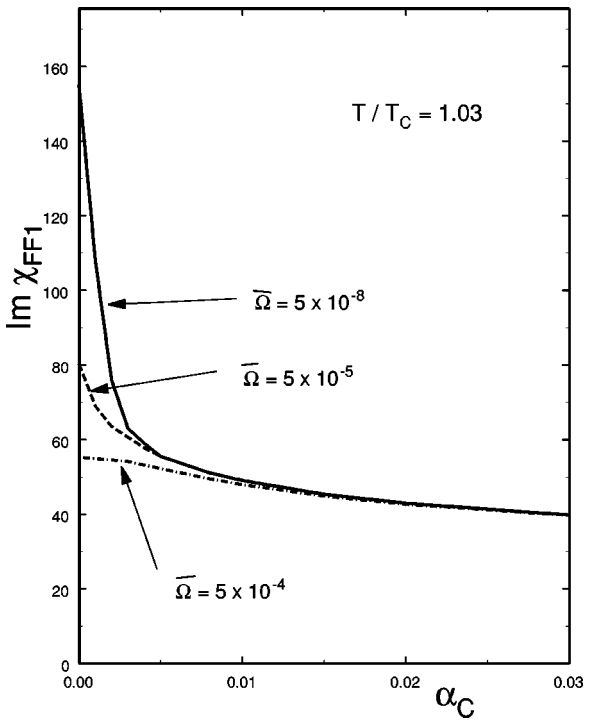

FIG. 5. The fluctuation contribution $\mathrm{Im}\,\chi^{(1)}_{FF,\Gamma}(\omega)$ measured in units of $[(a/\xi_0)^2(\hbar\omega/E_F)N_0/2]$ as a function of the pair breaking parameter α_C for several values of the reduced external frequency $\bar{\Omega}=\hbar\omega/2E_F$. For the experimental value $\bar{\Omega}=5\times10^{-8}$ the effect of even very little pair breaking is drastic.

relative to T_C and T_{C0} moves away with increasing Γ. Thus the fluctuations at T would be expected to be rather independent of Γ. That $\mathcal{D}$ actually increases arises mathematically from the dependence of the ln term in Eq. (31) on Γ in this case. The effect of pair breaking in the single-particle propagators, however, leads to a decrease of the susceptibility diagrams which usually dominates over the effect arising from $\mathcal{D}$.

We consider first $\chi^{(1)}_{FF}$ since it is the dominant contribution without pair breaking and its limiting t dependence is qualitatively changed by the addition of pair breaking. Equations (15) and (16) are still valid if the frequencies are renormalized according to Eq. (29). The frequency sum and then the angular integrations can be carried out exactly with the result

$$\mathrm{Im}\,\chi^{(1)}_{FF\Gamma}(\omega)=\left[\left(\frac{a}{\xi_0}\right)^2\frac{\hbar\omega}{E_F}\frac{N_0}{2}\right]I_\Gamma, \tag{33}$$

$$I_\Gamma=\frac{\varepsilon_c}{16\pi^4\bar{T}\bar{\Omega}}\int_0^\Lambda dx\,x\,\mathcal{D}(x)\int_{-\infty}^{+\infty}du\,f(2\pi u)\times Y(u,\eta,\alpha)[Y(u+\Omega,\eta,\alpha)-Y(u-\Omega,\eta,\alpha)], \tag{34}$$

where f is the Fermi function, $\eta=\varepsilon_c x/2\pi\bar{T}$, $\Omega=\hbar\omega/2\pi k_B T$, and

$$Y(a,b,c)=\pi\sqrt{2[(b^2-a^2+c^2+\sqrt{N})/N]^{1/2}},$$

with $N=(b^2-a^2+c^2)^2+4a^2c^2$. We have computed I_Γ numerically and the result as a function of the pair breaking parameter α_C is shown in Fig. 5 for several values of the external frequency, $\bar{\Omega}=\hbar\omega/2E_F$. Note the very large and rapid change at small pair breaking for the experimentally relevant frequency $\bar{\Omega}=5\times10^{-8}$.

Caculation of $\mathrm{Im}\,\chi^{(2)}_{FF}(\omega)$ for finite Γ yields

$$\mathrm{Im}\,\chi^{(2)}_{FF,\Gamma}(\omega)=\left[\left(\frac{a}{\xi_0}\right)^2\frac{\hbar\omega}{E_F}\frac{N_0}{2}\right]\left[\frac{\varepsilon_c}{\pi\bar{T}}\right]\times\int_0^\Lambda x\mathcal{D}(x)dx\int_0^{2\pi}d\phi_1\int_0^{2\pi}d\phi_2\times\sum_{n=0}^{\infty}\frac{1}{(\mu_2-\mu_1)^2+(4\pi\alpha_C)^2}\times\left\{\frac{[2\pi\alpha_C(\mu_1^2+p_{n+}^2)+(\mu_2-\mu_1)\mu_1 p_{n+}]}{(p_{n+}^2+\mu_1^2)^2}-\frac{[2\pi\alpha_C(\mu_2^2+p_{n-}^2)+(\mu_2-\mu_1)\mu_2 p_{n-}]}{(p_{n-}^2+\mu_2^2)^2}\right\}, \tag{35}$$

where $p_{n\pm}=p_n\pm2\pi\alpha_C/\bar{T}$. A similar calculation leads to the result that $\mathrm{Im}\,\chi_{GG,\Gamma}(\omega)$ is simply given by Eq. (23) with the replacement $p_n\to p_n+2\pi\alpha_C/\bar{T}$.

The limiting behavior of $\mathrm{Im}\,\chi_{GG,\Gamma}(\omega)$ and $\mathrm{Im}\,\chi^{(2)}_{FF,\Gamma}(\omega)$ for $t=(T-T_C)/T_C\to0$ is still given by Eq. (24). Similarly,

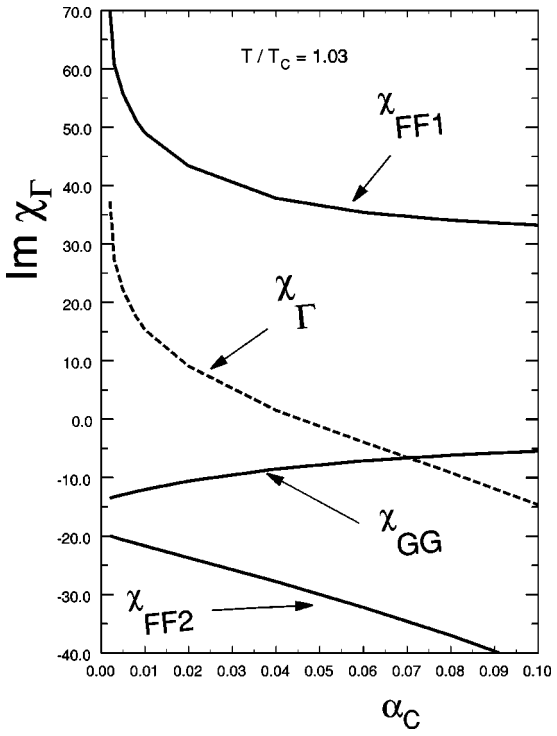

FIG. 6. The fluctuation contributions to $[1/(T_1T)]_{\mathrm{FL}}$, $\mathrm{Im}\,\chi_\Gamma(\omega)=\mathrm{Im}\,\chi^{(1)}_{FF,\Gamma}+\mathrm{Im}\,\chi^{(2)}_{FF,\Gamma}+\mathrm{Im}\,\chi^{(1)}_{GG,\Gamma}$, measured in units of $[(a/\xi_0)^2(\hbar\omega/E_F)N_0/2]$ as a function of the pair breaking parameter α_C for $T=1.03T_C$ and $\overline{\Omega}=\hbar\omega/2E_F=5\times10^{-8}$.

for finite Γ, the T dependence of $\mathrm{Im}\,\chi^{(1)}_{FF,\Gamma}(\omega)$ now also arises primarily from the integral of $x\mathcal{D}(x)$ in Eq. (34) and one finds $\mathrm{Im}\,\chi^{(1)}_{FF,\Gamma}(\omega)\propto-\ln t$, for $t\to0$. Thus, in the presence of pair breaking, the magnitudes of all three contributions have the same limiting temperature dependence.

In Fig. 6 we plot the fluctuation contribution to $[1/(T_1T)]_{\mathrm{FL}}$, $\mathrm{Im}\,\chi_\Gamma(\omega)$, given by Eqs. (1) and (2), vs α_C. Note that $\mathrm{Im}\,\chi^{(2)}_{FF,\Gamma}$ increases in magnitude with increasing α_C until it dominates over $\mathrm{Im}\,\chi^{(1)}_{FF,\Gamma}$ leading to a change of sign of the total contribution (dotted line) for the pair breaking parameter α_C near 0.05. This effect also occurs in the presence of weak elastic scattering.[21] In Fig. 7(a) we plot the total contribution vs T/T_C for a range of α_C from 0 to 0.1. The detailed plots in Figs. 7(b) and 7(c), for small and large α_C, show the dominance of $\mathrm{Im}\,\chi^{(2)}_{FF,\Gamma}$ for large pair breaking, yielding a negative divergence. We point out that, in the presense of inelastic scattering (pair breaking), our results here in the exact clean limit are qualitatively similar to those with weak elastic scattering.[21]

To summarize briefly, we have shown that the Maki diagram in 2D is pathological in the exact clean limit but the divergences occur for a different reason than in the usual dirty limit. In the presence of pair breaking due to inelastic scattering, which of course will always be present to some extent, reasonable results are obtained. A small amount of pair breaking also strongly reduces the increase in T_1^{-1} as T_C is approached. We have also seen that pair breaking in the fluctuation propagator $\mathcal{D}$ can affect T_1^{-1} quite differently than pair breaking in the Green's functions in the remainder of the diagram. In $\mathrm{Im}\chi^{(1)}_{FF,\Gamma}(\omega)$, for example, the increase in T_1^{-1} due to pair breaking in $\mathcal{D}$ is more than compensated for by the decrease arising from the Green's functions.

The strong effect of even a very small amount of pair breaking within our simple weak-coupling model underlines the need for a strong-coupling Eliashberg calculation including inelastic scattering due to boson exchange before quantitative comparison with experiment can be attempted for specific systems.

III. EFFECT OF BKT VORTEX-ANTIVORTEX FLUCTUATIONS ON T_1^{-1} AND T_2^{-1}

Up to now we have discussed the effect of Gaussian fluctuations of the order parameter on the NMR relaxation rate T_1^{-1} near the mean-field transition temperature T_{C0} of a 2D superconductor. The weakly coupled 2D layers of high-T_C superconductors promote the formation of topological excitations in the form of pancake vortex-antivortex pairs associated with the singular part of the phase field of the complex order parameter. Neglecting Josephson coupling, these VA excitations reduce the transition temperature to a Berezinskii-Kosterlitz-Thouless[31] transition temperature T_{BKT}, above which the bound pairs start to break up into free vortices and antivortices. We now proceed to study the effect of magnetic-field fluctuations caused by the translational motions of vortices and antivortices on T_1^{-1} and T_2^{-1} in the vicinity of T_{BKT}.

A. Vortex fluctuations in BKT theory

In thin superconducting films, BKT theory[31] predicts that below a transition temperature T_{BKT} spontaneously created pancake vortices and antivortices are bound in pairs with zero total magnetic flux and do not destroy the off-diagonal quasi-long-range order. Above T_{BKT}, the large pairs break up into free vortices and antivortices, which are responsible for the dissipation of electrical currents, and quasi-long-range order is lost. Around T_{BKT} there is a vortex-antivortex fluctuation regime. The time and distance behaviors of these fluctuations affect the transport properties; e.g., BKT behavior is clearly seen at microwave frequencies[7] and in the dc current-voltage characteristics. This picture is essentially unchanged in layered superconductors if the Josephson coupling is ignored.[32,5] (Under ''Josephson coupling'' one understands *all* interlayer pair transitions contributing to the Josephson current.)

In weakly coupled high-T_c superconductors such as $Bi_2Sr_2CaCu_2O_{8+\delta}$ (Bi-2212) the results are changed, since the pancake vortices in the layers become connected by Josephson vortices between the layers.[33,6,3,5] The Josephson vortices lead to a linear term in the interaction of pancakes connected in this way. The general picture is the following[3,4]: The VA pairs start to unbind at a BKT temperature T_{BKT}, but the linear interaction leads to confinement of the pairs at a length scale Λ, called the Josephson length. The BKT renormalization is cut off at pair sizes of the order of Λ. Very close to T_{BKT}, where the BKT correlation length ξ_{BKT} exceeds Λ, the interlayer coupling becomes important

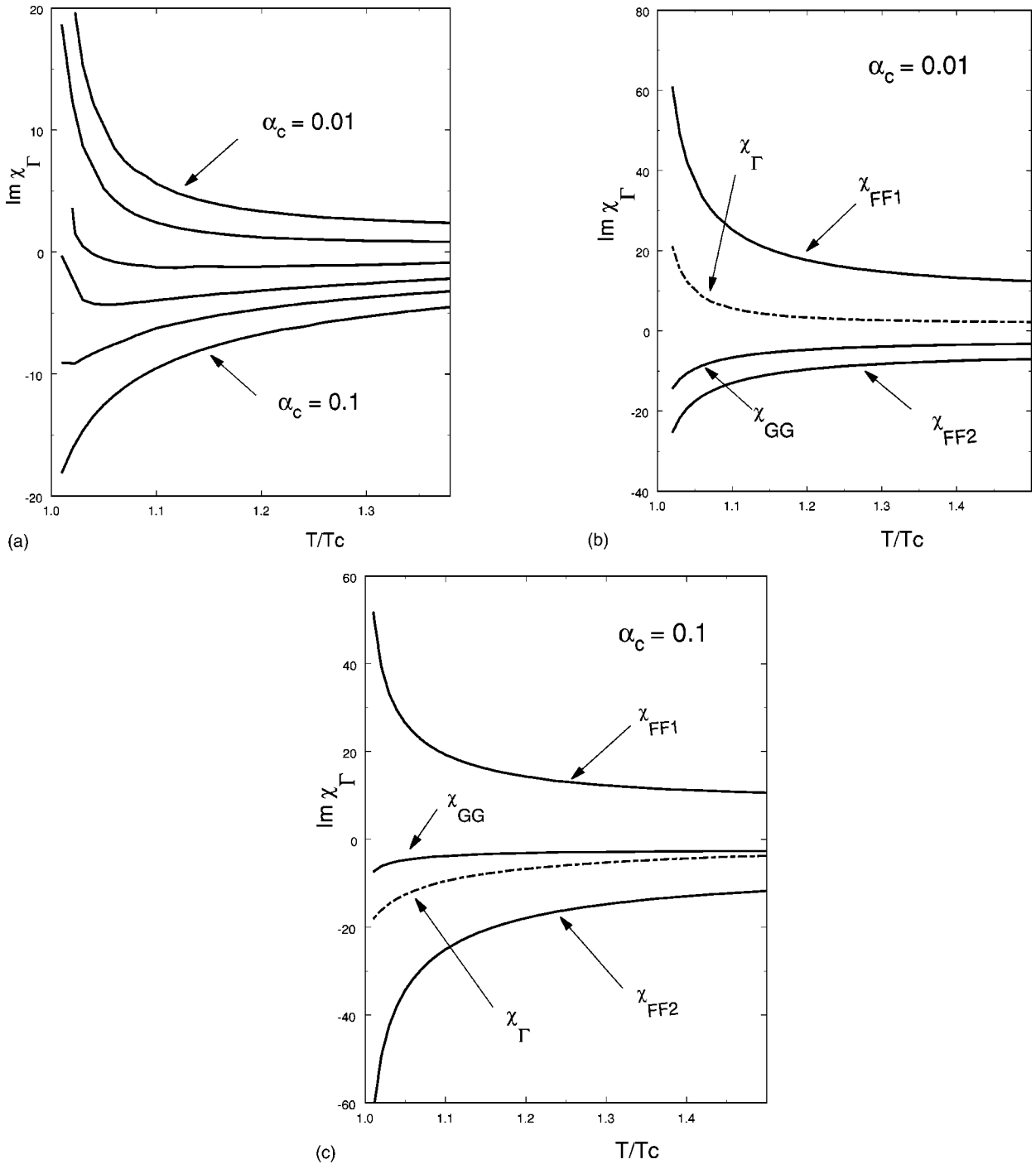

FIG. 7. The fluctuation contribution to $[1/(T_1T)]_{\mathrm{FL}}$, Im $\chi_\Gamma(\omega)$, measured in units of $[(a/\xi_0)^2(\hbar\omega/E_F)N_0/2]$ as a function of temperature for a range of the pair breaking parameter $\alpha_C=0.01$, 0.02, 0.04, 0.06, 0.08, and 0.10 (from top to bottom) and $\bar{\Omega}=\hbar\omega/2E_F=5\times10^{-8}$. The details for small and large pair breaking are shown in (b) and (c).

and the system shows three-dimensional critical behavior.[34] The true transition takes place at a temperature T_C. At a higher temperature, where the BKT correlation length $\xi_{\mathrm{BKT}}(T)$ falls below Λ, 2D fluctuations become important again and remain essential up to T_{C0}, where the local condensation energy vanishes. Critical fluctuations shift T_{C0} slighty downwards from the mean-field value. Around T_C there is a narrow 3D critical regime in which fluctuating vortex loops through more than a single layer are crucial. We are considering weakly coupled high-T_C superconductors in the sense that this 3D critical region is much narrower than the 2D fluctuation regime, which is well described by BKT theory. We therefore neglect the Josephson coupling and restrict ourselves to the 2D fluctuation region.

In the following we are concerned with the effect of BKT VA fluctuations on the spin-lattice relaxation rate T_1^{-1} and the spin-spin relaxation rate T_2^{-1}. Up to now, the experiments on BKT fluctuations consist mainly of flux-noise

measurements[35,36] with frequencies of the order of $\omega \sim 10^4\ \mathrm{s}^{-1}$, whereas NMR and NQR spectroscopies are characterized by frequencies of order 10^7–$10^8\ \mathrm{s}^{-1}$.

B. Vortex relaxation mechanisms

We discussed above the microscopic contributions to the relaxation rates arising from superconducting quasiparticles in the regime of Gaussian fluctuations. Now we proceed to study the macroscopic contributions of fluctuations due to VA excitations. The vortices cause contributions from both the quasiparticle excitations in their normal cores and from the fluctuating magnetic fields carried by them. These fluctuating fields interact directly with the nuclear magnetic moments and cause spin-flip transitions. The nuclear spins in the vortex cores and in the superconducting regions can be brought into thermal equilibrium by cross relaxation through simultaneous spin flips of neighboring nuclei, i.e., by spin diffusion. In type-II superconductors, the cross relaxation of the nuclear spins in the normal core with the nuclei not in the core tends to be suppressed by the mismatch of the Zeeman energies in an inhomogeneous magnetic field.[37] However, in high-T_c superconductors in the absence of an external field cross relaxation is apparently not suppressed by this effect. The experimentally observed line width, of the order of T_2^{-1}, is about $10^5\ \mathrm{s}^{-1}$. On the other hand, the magnetic field variations due to the vortices and the corresponding variation of Zeeman energies of the ^{63}Cu nuclei lead to an inhomogeneous line width which is much smaller, of the order of $10^3\ \mathrm{s}^{-1}$.[38] Hence the system is homogeneous; the ^{63}Cu nuclei can be considered as a single system subject to different relaxation mechanisms. Furthermore, the motion of the vortex cores, which visit many nuclei, also homogenizes the spin system.

We now focus on the relaxation of nuclear spins caused by the fluctuating magnetic fields of the VA pairs. Since a static magnetic field is not easily taken into account in BKT theory, effects of BKT vortex fluctuations are best studied in the relaxation rates measured in nuclear *quadrupole* resonance experiments on ^{63}Cu nuclei which have spin $I=3/2$ and nuclear quadrupole moment $Q=-0.157\times10^{-24}\,\mathrm{cm}^2$. The local electric field gradient is oriented in the z direction and gives a quadrupolar splitting that is much larger than the Zeeman splitting due to the magnetic field of the vortices. The relaxation rates are governed by the time-dependent correlation functions of the magnetic field, which are determined by the VA fluctuations. The evaluation of these correlation functions for the diffusing and recombining vortices is the main task. We then proceed to discuss the NQR relaxation rates in terms of the magnetic-field fluctuations.

C. Magnetic-field correlation functions

The Redfield theory gives the nuclear spin relaxation rates in terms of correlation functions of the fluctuating magnetic field.[38,39] We are interested in the correlation functions for the time-dependent local magnetic field in a given layer,

$$k_{\alpha\beta}(t)\equiv\overline{h_{n,\alpha}(\mathbf{r},t)h_{n,\beta}(\mathbf{r},0)}=\overline{h_{0,\alpha}(0,t)h_{0,\beta}(0,0)}, \quad (36)$$

where $h_{n,\alpha}(\mathbf{r},t)$ is the α component of the magnetic field at point $\mathbf{r}$ and time t in layer n. This field originates from the VA pairs in all the layers and is given by

$$\mathbf{h}_0(0,t)=\sum_n\sum_{\nu=1}^{N}[\mathbf{H}_{-n}(-\mathbf{r}_{-n,\nu+}(t))-\mathbf{H}_{-n}(-\mathbf{r}_{-n,\nu-}(t))], \quad (37)$$

where $\mathbf{r}_{n,\nu+}(t)$ and $\mathbf{r}_{n,\nu-}(t)$ are the positions of the vortex and antivortex of the νth pair in layer n at time t, and $\mathbf{H}_n(\mathbf{r})$ is the magnetic field in layer n at $\mathbf{r}$ of a single vortex centered at the origin. The components of this field parallel and perpendicular to the layers are[40,41]

$$\mathbf{H}_{n\parallel}(\mathbf{r})=\frac{\phi_0 s\mathbf{r}}{4\pi\lambda_{ab}^2 r^2}\mathrm{sgn}(n)\left[\exp\left(-\frac{|n|s}{\lambda_{ab}}\right)-\frac{|n|s}{\sqrt{r^2+n^2s^2}}\exp\left(-\frac{\sqrt{r^2+n^2s^2}}{\lambda_{ab}}\right)\right], \quad (38)$$

$$H_{n,z}(\mathbf{r})=\frac{\phi_0 s}{4\pi\lambda_{ab}^2\sqrt{r^2+n^2s^2}}\exp\left(-\frac{\sqrt{r^2+n^2s^2}}{\lambda_{ab}}\right). \quad (39)$$

Here $\phi_0=hc/2e$ is the flux quantum, λ_{ab} is the penetration depth inside the layer, and s is the interlayer separation. Whereas the z component is of short range in both the in-plane and the z direction, the in-plane component is of short range only in the z direction and falls off with $1/r$ in the plane. For the convenient evaluation of the relaxation rates we will later use the Fourier transforms

$$\mathbf{H}_{n\parallel}(\mathbf{k})=i\frac{\phi_0 s\mathbf{k}}{4\pi\lambda_{ab}^2 k^2}\exp(-|n|s\sqrt{k^2+\lambda_{ab}^{-2}}), \quad (40)$$

for $n\neq0$, $\mathbf{H}_{0\parallel}(\mathbf{k})=0$, and

$$H_{n,z}(\mathbf{k})=\frac{\phi_0 s}{4\pi\lambda_{ab}^2}\frac{1}{\sqrt{k^2+\lambda_{ab}^{-2}}}\exp(-|n|s\sqrt{k^2+\lambda_{ab}^{-2}}). \quad (41)$$

We take the correlations between the fields of the vortex and the antivortex of the same pair into account but neglect interpair correlations. This is a good approximation, since the typical pair size is small compared with the average distance between pairs below the transition and even in a significant temperature range above it.[42] In the following we are only interested in the diagonal components of $k_{\alpha\beta}$. They can be written as

$$k_{\alpha\alpha}(t)=\frac{2N}{F}\sum_n\int d^2r'_+\,d^2r'_-\,d^2r_+\,d^2r_-\,H_{-n,\alpha}(-\mathbf{r}'_+)\times[H_{-n,\alpha}(-\mathbf{r}_+)-H_{-n,\alpha}(-\mathbf{r}_-)]\times P(\mathbf{r}'_+,\mathbf{r}'_-;\mathbf{r}_+,\mathbf{r}_-;t)f(\mathbf{r}_+-\mathbf{r}_-). \quad (42)$$

Here, we assume the presence of N vortices and N antivortices in each layer so that $N/F\equiv n$ is the vortex density calculated as a function of temperature in Refs. 42 and 38. The

function $f(\mathbf{r})$ gives the normalized size distribution of the pairs. The *diffusion function* P describes the motion of the pairs within a layer. We now discuss the functions P and f.

We assume diffusive motion of vortices but take the intrapair interaction into account. The diffusion function P is defined as follows: $P(\mathbf{r}'_+,\mathbf{r}'_-;\mathbf{r}_+,\mathbf{r}_-;t)d^2r'_+\,d^2r'_-$ is the probability of finding the vortex of a given pair in the area $d^2r'_+$ about $\mathbf{r}'_+$ and the antivortex of the same pair in $d^2r'_-$ about $\mathbf{r}'_-$ at time t, provided the vortex was at $\mathbf{r}_+$ and the antivortex at $\mathbf{r}_-$ at $t=0$. The diffusion function P is discussed in a recent paper by Timm[43] in the context of flux noise. Here we summarize the results. Assuming for the moment that vortices and antivortices are unbound, P is simply a product of free diffusion functions for $\mathbf{r}_+$ and $\mathbf{r}_-$ with a diffusion constant D. It can be rewritten as

$$P\left(\mathbf{R}'+\frac{\mathbf{r}'}{2},\mathbf{R}'-\frac{\mathbf{r}'}{2};\mathbf{R}+\frac{\mathbf{r}}{2},\mathbf{R}-\frac{\mathbf{r}}{2};t\right)$$
$$=\frac{1}{2\pi Dt}\exp\left(-\frac{|\mathbf{R}'-\mathbf{R}|^2}{2Dt}\right)$$
$$\times\frac{1}{8\pi Dt}\exp\left(-\frac{|\mathbf{r}'-\mathbf{r}|^2}{8Dt}\right), \tag{43}$$

which is the product of free diffusion functions for the center of mass $\mathbf{R}$ and the separation vector $\mathbf{r}$ of a pair, showing that the center of mass and the separation vector diffuse with $D_{\rm cm}=D/2$ and $D_{\rm rel}=2D$, respectively. The assumption of unbound pairs would be justified for a small density of essentially free vortices, a situation that does not arise in practice. We take into account the interaction between vortex and antivortex, which is logarithmic in distance r, $V(r)\approx q^2\ln(r/r_0)$, where q is the charge of the vortex in the Coulomb gas model and r_0 can be chosen as the size of the vortex core, and solve the Fokker-Planck diffusion equation. The result is

$$P\left(\mathbf{R}'+\frac{\mathbf{r}'}{2},\mathbf{R}'-\frac{\mathbf{r}'}{2};\mathbf{R}+\frac{\mathbf{r}}{2},\mathbf{R}-\frac{\mathbf{r}}{2};t\right)$$
$$=\frac{1}{2\pi Dt}\exp\left(-\frac{|\mathbf{R}'-\mathbf{R}|^2}{2Dt}\right)P_{\rm rel}(\mathbf{r}',\mathbf{r};t), \tag{44}$$

where the first term accounts for the motion of the center of mass and $P_{\rm rel}$ gives the relative motion in polar coordinates r, ϕ,

$$P_{\rm rel}=\frac{1}{4\pi D_{\rm rel}t}\left(\frac{r'}{r}\right)^{\gamma}\exp\left(-\frac{r'^2+r^2}{4D_{\rm rel}t}\right)$$
$$\times\sum_{n=-\infty}^{\infty}e^{in(\phi'-\phi)}I_{\sqrt{\gamma^2+n^2}}\left(\frac{rr'}{2D_{\rm rel}t}\right). \tag{45}$$

Here, $\gamma=(1-q^2/k_BT)/2$ and $I_\mu(x)$ is a modified Bessel function. Note that P incorporates the effect of pair recombination: Pairs with zero separation are taken out of the process. Thus P starts out normalized to unity at $t=0$ but then drops to zero on the time scale of the lifetime τ_r of a VA pair, determined by $D_{\rm rel}=2D$. Newly created VA pairs do not enter in $k_{\alpha\beta}$, since their positions are assumed to be uncorrelated to those of existing pairs. If the diffusion of a vortex were limited only by the Bardeen-Stephen friction mechanism[44] (no pinning) with a large diffusion constant, τ_r would be much smaller than the time scale of NQR spectroscopy, of order 10^{-7}–10^{-8} s. We will come back to this problem below.

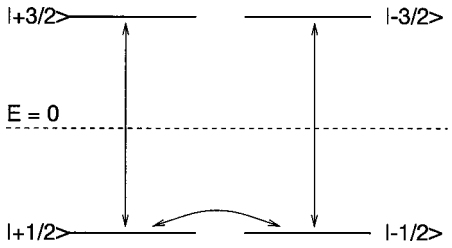

FIG. 8. Energy levels of ^{63}Cu nuclei in the CuO_2 layer due to quadrupolar splitting. The allowed transitions are indicated by arrows.

Besides the diffusion function, the correlation function in Eq. (42) contains the distribution function of pair sizes, $f(r)$. Taking into account that the magnetic field of a vortex changes on the scale of the penetration depth λ_{ab}, and that for this reason the fields of a vortex and an antivortex almost cancel for separations $r\ll\lambda_{ab}$, we approximate the pair distribution function with an analytical expression that becomes exact for large pairs and does not introduce irrelevant complications for small r,

$$f(r)\propto\frac{1-(r/r_0)^2}{1-(r/r_0)^{2\zeta+6}}, \tag{46}$$

which should be normalized to unity. The form of the exponent ζ is given in Ref. 43. We only note that ζ vanishes for $T\geqslant T_c$ and is positive and, to leading order, proportional to $(T_c-T)^{1/2}$ below T_c, where we now denote the BKT transition temperature by T_c.

D. NQR relaxation rates

We can now evaluate the NQR relaxation rates in terms of the correlation functions, Eq. (42). The NQR rates are of interest here because the BKT vortex fluctuations show up more clearly in the absence of Abrikosov vortices due to an external magnetic field. In a vanishing field, however, the occupation of the quadrupolar energy levels cannot be described in terms of a Boltzmann distribution with a spin temperature and, therefore, we proceed by calculating the NQR relaxation rates using the Bloch-Wangsness-Redfield theory.[45] We can apply this theory, since the interaction between the nuclear spins and the magnetic field of the vortices is a small perturbation compared with the quadrupolar splitting. The energy levels of in-plane ^{63}Cu nuclei due to quadrupole splitting are shown in Fig. 8. Since the field gradient is oriented along the z direction and $I=3/2$, the relaxation rates are given by

$$T_1^{-1}=\sqrt{\pi/2}\,\gamma_n^2[9k_{xx}(0)-7k_{xx}(\omega)], \tag{47}$$

$$T_2^{-1}=\sqrt{\pi/2}\gamma_n^2\left[\frac{1}{4}k_{xx}(\omega)+\frac{3}{4}k_{xx}(0)+k_{zz}(0)\right], \quad (48)$$

where $\gamma_n=7.1\ \mathrm{G}^{-1}\,\mathrm{s}^{-1}$ is the gyromagnetic ratio of the ^{63}Cu nuclei and $\omega=|\omega_{+3/2}-\omega_{+1/2}|=|\omega_{-3/2}-\omega_{-1/2}|$. The correlation function given by the temporal Fourier transform of Eq. (42) has the form

$$\begin{aligned}k_{\alpha\alpha}(\omega)=&\frac{2N}{F}\frac{8\sqrt{2\pi}}{D_{\mathrm{rel}}}\int d^2k\sum_n |H_{-n,\alpha}(\mathbf{k})|^2\int_0^\infty dr\, r^{1-\gamma}f(r)\\ &\times\sum_{m=1,\mathrm{odd}}^{\infty}J_m(kr/2)\int_0^\infty dr'\,r'^{1+\gamma}J_m(kr'/2)\\ &\times\mathrm{Re}\,I_{\sqrt{\gamma^2+m^2}}(\sqrt{k^2/4+i\omega/D_{\mathrm{rel}}}\,r_<)\\ &\times K_{\sqrt{\gamma^2+m^2}}(\sqrt{k^2/4+i\omega/D_{\mathrm{rel}}}\,r_>),\end{aligned} \quad (49)$$

where J, K, and I are Bessel functions, $\alpha=x,y,z$, $r_<=\min(r,r')$, and $r_>=\max(r,r')$. This equation shows how the spectral density of the magnetic-field fluctuations determines the relaxation rates, Eqs. (47) and (48). With the Fourier transforms of the vortex magnetic field substituted from Eqs. (40) and (41), the final form of the correlation functions is

$$\begin{aligned}k_{xx}(\omega)=&\frac{2N}{F}\frac{4\sqrt{2\pi}}{D_{\mathrm{rel}}}\frac{\phi_0^2 s^2}{4\pi\lambda_{ab}^4}\\ &\times\int_0^\infty\frac{dk}{k}\frac{1}{\exp(2s\sqrt{k^2+\lambda_{ab}^{-2}})-1}\int_0^\infty dr\, r^{1-\gamma}f(r)\\ &\times\sum_{m=1,\mathrm{odd}}^{\infty}J_m(kr/2)\int_0^\infty dr'\,r'^{1+\gamma}J_m(kr'/2)\\ &\times\mathrm{Re}\,I_{\sqrt{\gamma^2+m^2}}(\sqrt{k^2/4+i\omega/D_{\mathrm{rel}}}\,r_<)\\ &\times K_{\sqrt{\gamma^2+m^2}}(\sqrt{k^2/4+i\omega/D_{\mathrm{rel}}}\,r_>)\end{aligned} \quad (50)$$

and $k_{zz}(\omega)$ follows with a similar form.

The effect of motional narrowing is taken into account: The nuclei are fixed and experience the field fluctuations of the vortices as they pass by. An important parameter for diffusive relaxation phenomena is the characteristic frequency ω_c corresponding to the inverse jump time for the diffusion process.[46] Here, $\omega_c\sim D_{\mathrm{rel}}/4\lambda_{ab}^2$, the reason being that the dependence on ω is determined by $k^2/4+i\omega/D_{\mathrm{rel}}$ and the characteristic value of k is $1/\lambda_{ab}$. By inspection of $k_{\alpha\alpha}(\omega)$ it is seen that the correlation function becomes really frequency dependent only for frequencies $\omega>\omega_c$. The Fourier transform $k_{\alpha\alpha}(t)$, Eq. (36), begins to decrease for $t<1/\omega_c$. However, $k_{\alpha\alpha}(t)$ does not have the simple exponential decay form characteristic for the case of nuclei diffusing in a static, random magnetic field.

For the special case of unbound pairs, see Eq. (43), the result for T_1^{-1} takes the simple form[47]

$$\begin{aligned}T_1^{-1}=&\frac{3\gamma_n^2 n_P\phi_0^2}{4\pi}\frac{D}{\omega^2\lambda_{\mathrm{eff}}^2}\int_0^{1/\xi_{ab}}dk\frac{k}{1+D^2k^4/\omega^2}\\ &\times[\exp(2s\sqrt{k^2+\lambda_{ab}^{-2}})-1]^{-1},\end{aligned} \quad (51)$$

where n_P is the temperature-dependent pair density, $\lambda_{\mathrm{eff}}=2\lambda_{ab}^2/s$ is the effective penetration depth,[3,4] and ξ_{ab} is the in-plane coherence length. In the general case there is no such simple form. We now proceed to discuss the results in terms of the diffusion constant D.

E. BKT vortex fluctuations, T_1^{-1}, and T_2^{-1}

The most important parameter in Eq. (50) is the diffusion constant $D_{\mathrm{rel}}=2D$ that governs both the free motion of independent vortices and the motions of a vortex and an antivortex towards each other, leading eventually to their recombination. In the absence of pinning, D is given by the Bardeen-Stephen formula[44]

$$D=D_0\equiv\frac{2\pi c^2\xi_{ab}^2\rho_n k_B T}{\phi_0^2 d}, \quad (52)$$

where ρ_n is the normal-state resistivity and d is the layer thickness. For Bi-2212, D_0 is of the order of 1 cm^2/s at low temperatures.[48] This value is so large that vortices and antivortices would recombine so fast that there is no time left for a large number of nuclear relaxation processes to occur. Futhermore, also when ignoring recombination processes, the free motion of vortices and antivortices is so fast that the rapidly changing magnetic fields at the nuclei lead to slow relaxation, similar to the case of motional narrowing.

Slow diffusion rates and correspondingly long VA recombination times are crucial for obtaining measurable contributions to T_1^{-1} and T_2^{-1}. In real high-T_c superconductors there are always inhomogeneities, i.e., doping defects or intrinsic crystalline defects (twin boundaries, grain boundaries), which can pin vortices by their interaction with the normal vortex cores. A measure of the strength of the pinning potential is the energy E_p for the thermally activated motion of a vortex. Pinning leads to an Arrhenius-type temperature dependence

$$D=D_0\exp\left(-\frac{E_p}{k_B T}\right). \quad (53)$$

In terms of D the mean time between flights, or the time of stay, is given by $\tau_p=l_{\mathrm{eff}}^2/4D$, where l_{eff} is a measure of the flight distance.[49] Experimentally, D has been determined for different thicknesses of layered CuO_2 systems. For a one-unit-cell-thick film of Bi-2212, Rogers *et al.*[35] measured the low-frequency flux noise S_ϕ near T_c. By analyzing the frequency dependence of S_ϕ in terms of diffusion noise, the authors determined a characteristic frequency $\omega_c=D(T)/2\langle r\rangle^2$, above which $S_\phi\propto\omega^{-3/2}$; $\langle r\rangle$ is the average pair size. From these experiments the authors determined $D(T)$, Eq. (53), and find a temperature-dependent activation energy for a single CuO_2 layer, $E_p(T)\approx E_0(1-T/T_{c0})$, with $E_0/k_B\approx 800$ K. For more than one layer thick epitaxial

blocks of $DyBa_2Cu_3O_{7-x}$, the activation energy E_p is proportional to the number of layers, N, and begins to saturate at $N=3$ to $N=4$.[50] This is taken as direct evidence that the pancakes in two adjacent layers are coupled due to the Josephson effect and move as entities. With N up to 10^5, large activation energies $E_p \approx 8$ eV (consisting of the nucleation energy plus the pinning energy) are observed in epitaxial films of Bi-2212, where a BKT transition is experimentally found in the temperature dependence of the penetration depth.[51] In such crystals, the BKT transition may be driven by thermally created pairs of VA *lines* through several layers.

To sum up, the diffusion constant D for a pancake vortex in a single clean CuO_2 layer is large, $D \sim 1$ cm^2/s, so that the VA lifetime is short. However, in the real multilayer systems where the BKT transition is observed,[51,52] D can be small and thereby enhance the lifetime of a VA pair so that the relaxation of nuclear spins can accompany the translational diffusion of these pairs. The actual value of D can vary over many orders of magnitude; for this reason we treat D as an open parameter in the following discussion.

Let us first comment on T_1^{-1}, ignoring the interaction and recombination of VA pairs; cf. Eq. (51). We assume a multilayer structure of alternating single layers of $YBa_2Cu_3O_{7-x}$ and $PrBa_2Cu_3O_{7-x'}$; the distance between the superconducting CuO_2 layers is $s=24$ Å. Using $\lambda_{ab} \approx 1400$ Å, $\xi_{ab} \approx 12$ Å, and taking the experimental value $D=2\times10^{-4}$ cm^2/s, measured by Fiory *et al.*,[53] for a thin film of $YBa_2Cu_3O_{7-x}$ near T_c, we get from Eq. (51) a rate of $T_1^{-1} \approx 572\,\mathrm{s}^{-1}$, which is comparable with the experimental values.

Next, let us take into account the interaction and recombination of vortices and antivortices. The time it takes for a vortex to move to its nearest antivortex depends on the VA separation and on D for the single-vortex motion. Since D is not known, we evaluate the relaxation rates T_1^{-1} and T_2^{-1} as functions of the diffusion constant of the separation vector, $D_{\mathrm{rel}}=2D$. The curves shown in Fig. 9 are obtained by numerical integrations from Eqs. (47)–(49) using parameter values that apply to Bi-2212. The magnetic penetration depth and the Ginzburg-Landau coherence length are given by $\lambda_{ab}(T)/\lambda_{ab}(0)=\xi_{ab}(T)/\xi_{ab}(0)=\sqrt{T_{c0}/(T_{c0}-T)}$, where $\lambda_{ab}(0) \approx 2000$ Å, $\xi_{ab}(0) \approx 21.5$ Å, and $T_{c0} \approx 86.8$ K is the mean-field transition temperature. The distance between layers is $s \approx 15.5$ Å. The parameter $\gamma=(1-q^2/k_BT)/2$ depends on the VA interaction, $q^2=q_0^2(T_c-T)$, where $k_BT_c/q_0^2 \approx 0.2053$ and for T_c we take the value 84.7 K.[38] Figure 9 shows that the prefactor $1/D_{\mathrm{rel}}$ in Eq. (49) dominates the dependence of both relaxation rates on D_{rel}; both rates fall off approximately as $1/D_{\mathrm{rel}}$. The reason is that a large value of D_{rel} leads to fast recombination.[54] Then, the time-dependent correlation functions $k_{\alpha\alpha}(t)$ are narrow and their Fourier transforms $k_{\alpha\alpha}(\omega)$, Eq. (49), are broad and quite small even at $\omega \approx 0$. Hence, small diffusion constants are necessary to observe contributions from VA fluctuations to the relaxation rates.

The diffusion constant has an exponential temperature dependence if there are pinning effects. The corresponding

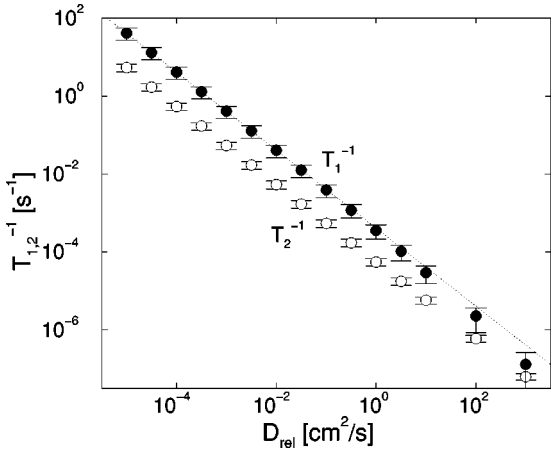

FIG. 9. The contributions of vortex-antivortex magnetic-field fluctuations to the longitudinal and transverse relaxation rates T_1^{-1} and T_2^{-1} as a function of the diffusion constant $D_{\mathrm{rel}}=2D$. The dotted line gives the contribution from $k_{xx}(\omega=0)$ to T_1^{-1}, corresponding to the first term on the right hand side of Eq. (47). The parameters used in Eqs. (47)–(49) are given in the text.

temperature dependences of T_1^{-1} and T_2^{-1} are evaluated with D from Eq. (53), using for $E_p(T)$ the experimental results of Rogers *et al.*[35] The bare diffusion constant D_0 is given by Eq. (52); it depends on T through ξ_{ab} and ρ_n, the normal resistance of a single layer. The experimental value of $D(T_c)$ is large, not much smaller than 1 cm^2/s. Assuming the experimental values of $D(T)$ obtained by Rogers *et al.*, the calculated relaxation rates in the vicinity of $T_c=84.7$ K are shown in Figs. 10 and 11. It is found that the temperature dependences of both rates are qualitatively similar to the quasiparticle contributions above and below T_c. There is a sharp drop of the rates below T_c. The vortex contribution to T_2^{-1} is smaller than the contribution to T_1^{-1}. Since the observed spin-spin relaxation rates are larger than the spin-lattice relaxation rates, the latter are more suitable for an experimental test.

The crucial point in our example is the small absolute values of the calculated relaxation rates. The numbers obtained by assuming a large value of D are several orders of

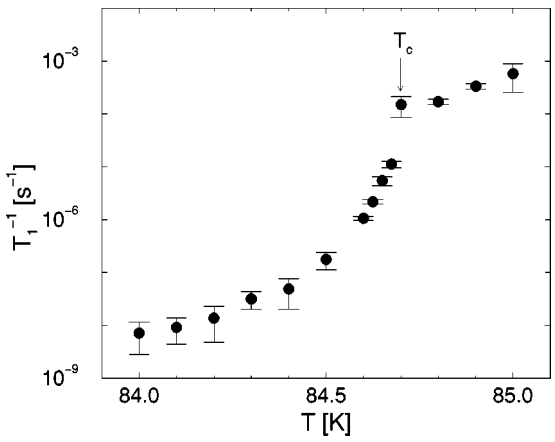

FIG. 10. Magnetic-field contribution to the longitudinal relaxation rate T_1^{-1} near T_c for Bi-2212.

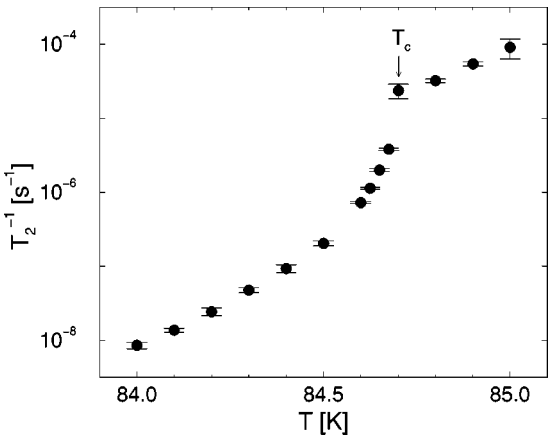

FIG. 11. Magnetic-field contribution to the transverse relaxation rate T_2^{-1} near T_c for Bi-2212.

magnitude smaller than the experimental values. These are of the order of 10^2–$10^3\,s^{-1}$ above T_c, where the relaxation is predominantly caused by quasiparticle excitations. Furthermore, we have mentioned above that quasiparticle excitations in the cores will also contribute to the relaxation effects from vortices. In a simple picture the vortex cores can be considered as normal-conducting regions, where normal-state-like excitations contribute to T_1^{-1} according to the Korringa law $(T_1T)^{-1}=K_0$; here K_0 is the Korringa constant in the normal state. In the superconducting state the vortex-core contribution to T_1^{-1} is approximately given by

$$\frac{1}{T_{1,\mathrm{core}}T}=2n_P(T)\pi\xi_{ab}^2(T)K_0, \tag{54}$$

where $2n_P$ is the areal density of vortices and $\pi\xi_{ab}^2$ is the area of one core. The calculated temperature dependence of $T_{1,\mathrm{core}}^{-1}$ for Bi-2212 is shown in Fig. 12. A very similar curve would result for $T_{2,\mathrm{core}}^{-1}$. The core contribution is much larger than the contribution from the VA magnetic-field fluctuations, Fig. 10.

There are, however, several effects that can make an experimental observation of the effect of the magnetic-field fluctuations feasible. We have already discussed possible mechanisms by which the diffusion constant D can become smaller—namely, pinning and coherent motion of stacks of vortices. Even if D is sufficiently small, however, the VA contribution to T_1^{-1} and T_2^{-1} is at best comparable with the quasiparticle contributions. In order to evade the in-plane quasiparticle effects, interplane ions can be used for NQR spectroscopy. The relaxation of interplane nuclear moments can be affected by the magnetic-field fluctuations originating from vortices and antivortices in the CuO_2 planes.[55] A possible candidate is ^{201}Hg in $HgBa_2CaCu_2O_{6+\delta}$ with the ^{201}Hg ion with spin $I=3/2$ and abundance 13.2% residing between two CuO_2 planes. So far NMR spectroscopy has been carried out only on the ^{199}Hg nucleus with $I=1/2$; an NMR spin-lattice relaxation time of $T_1=32$ ms is found at room temperature.[56] Although this value will increase with decreasing temperature if Korringa's relation applies, the relaxation rate T_1^{-1} at T_c could still be an order of magnitude larger than the contribution from magnetic-field fluctuations. Other interplanar candidates may be ^{87}Sr with $I=9/2$ and abundance 7% and ^{209}Bi with $I=9/2$ and abundance 100%, both in Bi-2212. The isotope ^{43}Ca($I=7/2$) is probably not a good candidate, since its abundance is rather small. To extend our approach to interplane ions, the sums over squared Fourier transforms of the vortex magnetic field in Eq. (49) have to be taken over the appropriate fractional values for n. There are other interplane ions with $I>1/2$ that are candidates for NQR relaxation measurements in order to observe the magnetic fields caused by the diffusional motion of BKT vortices. A pertinent question concerns the relative magnitudes of the magnetic fields at the interlayer sites that originate from VA fluctuations and from the fluctuating Cu moments in the CuO_2 planes, respectively.

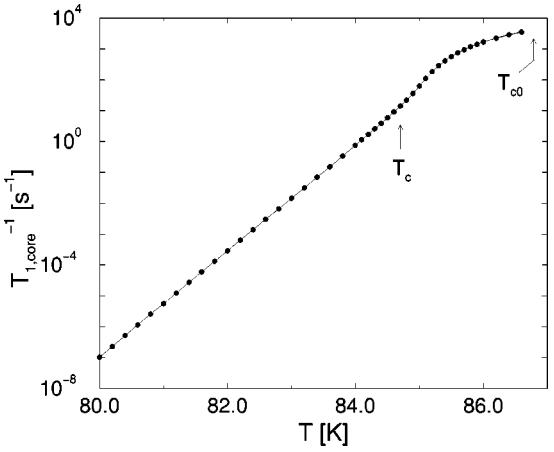

FIG. 12. Contribution to the longitudinal relaxation rate T_1^{-1} from vortex core relaxation.

IV. SUMMARY, CONCLUSIONS, AND COMMENTS ON EXPERIMENTS

In this paper we studied the effect of 2D superconducting fluctuations on the nuclear spin relaxation of layered superconductors above the superconducting transition temperature T_C and outside the region where Josephson coupling between the layers leads to a narrow 3D critical region surrounding T_C. Hence we model the superconductor as a set of 2D layers without interlayer coupling mechanisms that transfer Cooper pairs between adjacent layers. The fluctuations in each layer consist of the usual Gaussian fluctuations and the topological Berezinskii-Kosterlitz-Thouless[31] vortex-antivortex fluctuations. The Gaussian fluctuations are considered as the long-wavelength amplitude fluctuations of the superconducting order parameter and the BKT fluctuations are taken into account as the shorter-wavelength phase fluctuations of each layer. These two fluctuation effects dominate the superconducting fluctuation behavior in the 2D fluctuation regime (cf. Fig. 1) of layered systems.

We first evaluated in Sec. II, for *s*-wave superconductors, the effect of amplitude fluctuations on the hyperfine relaxation rate T_1^{-1} for pure systems, with and without pair breaking effects due to inelastic scattering. The amplitude fluctuations affect the Pauli spin susceptibility χ of the itinerant

charge carriers and thereby, via the hyperfine coupling, the decay of the nuclear polarization due to the spin-lattice relaxation. Our results for the relative effect of fluctuations on T_1^{-1} in zero magnetic field depend strongly on the pair breaking parameter $\alpha_C = \hbar/4\pi\tau_\phi k_B T_C$ as is seen from Figs. 6 and 7. The results for clean systems without pair breaking are given by Eqs. (24)–(26) and with pair breaking by Eqs. (33)–(35). Assuming small pair breaking effects, $\alpha_C \approx 0.01$, and the temperature just outside the critical region above T_C, say, $T > 1.01 T_C$, a fluctuation enhancement of T_1^{-1} occurs that is of order 10 with a slow decrease as the temperature moves away from T_C; see Fig. 7.

Let us comment on the feasibility of experimental verification of this enhancement effect and its temperature dependence. A difficulty can arise in observing this effect: The high-frequency fields used in NMR experiments on metals, and especially superconductors, are shielded within the penetration depth of the radio-frequency field.[57] For this reason most of the experiments are performed on powders with grain sizes smaller than the skin depth (in metals) or the penetration depth (in superconductors) or on thin films. In powders or thin films, however, the NMR lines are broadened by charge density fluctuations that emanate from crystal surfaces, an effect similar to the Friedel oscillations of the charge density surrounding an impurity in a simple metal.[58] This geometrical broadening effect will primarily affect the relaxation rate T_2^{-1} for nuclear spin-spin coupling, i.e., the natural line width. The charge fluctuations can also affect T_1^{-1} because of the change of the electron density at E_F. Hence, the singular behavior of T_1^{-1} near the transition, seen in Fig. 7, may be smeared out by surface effects.[59] Furthermore, the spread of *c*-axis orientations in powder samples can also smear the effect of fluctuations on T_1^{-1}.[20]

At this point one must ask what the chances are of finding systems in which these properties can be observed. Aside from possibily the electron-doped high-T_C superconductors mentioned in the Introduction, there are other quasi-2D superconductors with *s*-wave pairing and BCS behavior. The relaxation time T_1 of the ^{93}Nb nuclear spins in a single crystal of 2H-$NbSe_2$ (with trigonal prismatic coordination of the Nb atoms) has been measured by Wada.[60] The rate follows the Korringa relation in the normal state and increases exponentially in the superconducting state. Other dichalcogenides include the $TaS_{2-x}Se_x$ layer compounds which are BCS superconductors and can be intercalated with organic molecules to increase the interlayer separation to as much as 50 Å.[61] Finally there are the graphite intercalation compounds such as C_8K which are BCS superconductors with rather low T_C's.[62] One or the other of such quasi-2D systems may be a suitable candidate for observing the T_1 fluctuation effects discussed in this paper. The experimentalist may prefer to measure T_1 on a nucleus without a quadrupolar moment in order to avoid the line-broadening effect caused by electric field gradients near the metal surfaces of thin films or small particles.

In Sec. III we studied the effect of Berezinski-Kosterlitz-Thouless vortex-antivortex fluctuations on the NQR spin-lattice and spin-spin relaxation rates T_1^{-1} and T_2^{-1}, respectively. Here the symmetry of the superconducting order parameter will affect the field and current distributions of an individual vortex. However, for both *s*- and *d*-wave superconductors, the flux contained in a vortex is Φ_0, the magnetic field not too close to the vortex core does not depend on the symmetry of the order parameter, and, therefore, this symmetry will not affect the magnetic field fluctuations caused by the translational motions of an ensemble of VA pairs. Hence, the results for the relaxation rates T_1^{-1} and T_2^{-1} calculated in Sec. III can be applied to both *s*- and *d*-wave superconductors. One must keep in mind, however, that the relaxation processes of the VA pairs are not entirely the result of the translational diffusion processes. The relaxation processes due to quasiparticle excitations must also be taken into account and can be different for the two symmetries. We assume that clear experimental evidence exists for the BKT transition in quasi-two-dimensional systems, in particular for layered superconductors with weak interlayer coupling such as some high-T_C cuprates. We also assume that this coupling does not change the qualitative behavior of our results obtained for a stacked system of uncoupled layers. For uncoupled layers, the basic tenet of dynamical BKT behavior is that vortices and antivortices move diffusively with bonding and unbonding of pairs under the influence of random internal forces (pinning). We studied the effect of the fluctuating magnetic fields accompanying the motion of vortices and antivortices on the longitudinal and transverse NQR relaxation rates T_1^{-1} and T_2^{-1} in the vicinity of T_C. Our procedure uses a Coulomb gas description of thermally created VA pairs. The NQR relaxation rates were calculated in terms of the time-dependent correlation functions of the fluctuating magnetic field of the vortices and antivortices, Eq. (49). The interaction and recombination of VA pairs were taken into account and they can drastically reduce the correlation time. From the results obtained for T_1^{-1} and T_2^{-1}, Eqs. (47) and (48), it is seen that the vortex diffusion constant $D(T)$ plays a crucial role. The reason is that $D(T)$ determines both the translational motion of the vortices and also the recombination time of the VA pairs. From Figs. 9–11 it is seen that D must be sufficiently small in order to get contributions to the relaxation rates that are comparable to those caused by quasiparticle excitations. We discuss possible candidates for the experimental NMR spectroscopy of dynamical BKT effects in Sec. III. As for the interlayer quasiparticle contribution to the relaxation rates, one way to eliminate these contributions is to observe NQR on interlayer nuclei. Possible candidates are ^{87}SR and ^{209}Bi in Bi-2212 and ^{201}Hg in mercury cuprates. Also for NQR experiments on small particles or thin films, the surface effects can be important because the charge density oscillations induced by the surface will set up electric field gradients that can interact with the quadrupolar moments of the nuclei. Hence, an unambiguous observation of 2D fluctuation effects in NMR or NQR requires thoughtful experimental setups.

ACKNOWLEDGMENTS

We acknowledge helpful discussions with R. A. Klemm, J. Kötzler, and M. Pieper. C.T. acknowledges the support of the Deutsche Forschungsgemeinschaft.

[1] C.P. Slichter, in *Strongly Correlated Electronic Materials*, Los Alamos Symposium 1993, edited by K.S. Bedell *et al.* (Addison Wesley, New York, 1994); S.E. Barrett *et al.*, Phys. Rev. B **41**, 6283 (1990); A. Rigamonti, S. Aldrovani, F. Borsa, P. Carretta, F. Cintolesi, M. Corti, and S. Rubini, Nuovo Cimento A **16**, 1734 (1994).

[2] C.I. Halperin and D.R. Nelson, J. Low Temp. Phys. **36**, 1165 (1979).

[3] G. Blatter, M.V. Feigel'man, V.B. Geshkenbein, A.I. Larkin, and V.M. Vinokur, Rev. Mod. Phys. **66**, 1125 (1994).

[4] D.I. Glazman and A.E. Koshelev, Zh. Éksp. Teor. Fiz. **97**, 1371 (1990) [Sov. Phys. JETP **70**, 774 (1990)].

[5] C. Timm, Phys. Rev. B **52**, 9751 (1995).

[6] S.W. Pierson, Phys. Rev. Lett. **73**, 2496 (1994); **75**, 4674 (1995); Phys. Rev. B **51**, 6663 (1995); M. Friesen, *ibid.* **51**, 632 (1995); S.W. Pierson, M. Friesen, S.M. Ammirata, J.C. Hunnicut, and L.A. Gorham, *ibid.* **60**, 1309 (1999); S.W. Pierson and O.T. Valls, *ibid.* **61**, 663 (2000).

[7] J. Corson, R. Mallozzi, J. Orenstein, J.N. Eckstein, and I. Bosovic, Nature (London) **398**, 221 (1999).

[8] M.V. Ramallo and F. Vidal, Phys. Rev. B **59**, 4475 (1998); T. Tsusuki, J. Low Temp. Phys. **9**, 525 (1972); G. Blatter, B. Ivlev, and H. Nordborg, Phys. Rev. B **48**, 10 448 (1993).

[9] C.C. Tsuei and J.R. Kirtley, Phys. Rev. Lett. **85**, 182 (2000), recently presented phase sensitive evidence for *d*-wave symmetry in $Nd_{1.85}Ce_{0.15}CuO_{4-y}$.

[10] D. Manske, I. Eremin, and K.H. Bennemann, Phys. Rev. B **62**, 13 922 (2000).

[11] M. Weger, T. Maniv, A. Ron, and K.H. Benneman, Phys. Rev. Lett. **29**, 584 (1972).

[12] T. Maniv and S. Alexander, J. Phys. C **9**, 1699 (1976).

[13] K. Kuboki and H. Fukuyama, J. Phys. Soc. Jpn. **58**, 376 (1988).

[14] J. Heym, J. Low Temp. Phys. **89**, 869 (1992).

[15] J. Appel, D. Fay, and C. Kautz, J. Supercond. **7**, 607 (1994).

[16] J. Appel and D. Fay, J. Low Temp. Phys. **99**, 549 (1995).

[17] M. Randeria and A. Varlamov, Phys. Rev. B **50**, 10 401 (1994).

[18] A.A. Varlamov, G. Balestrino, E. Milani, and D.V. Livanov, Adv. Phys. **48**, 655 (1999).

[19] P. Carreta *et al.*, Phys. Rev. B **54**, R9682 (1996).

[20] P. Carreta, A. Lascialfari, A. Rigamonti, A. Rosso, and A. Varlamov, cond-mat/9911182 (unpublished).

[21] M. Eschrig, D. Rainer, and J.A. Sauls, Phys. Rev. B **59**, 12 095 (1999).

[22] T. Dahm, D. Manske, and L. Tewordt, Phys. Rev. B **55**, 15 274 (1997), have considered the GG/DOS diagram for the *d*-wave case within the strong-coupling FLEX approximation.

[23] C.H. Pennington *et al.*, Phys. Rev. B **39**, 274 (1989).

[24] K.R. Gorny *et al.*, Phys. Rev. Lett. **81**, 2340 (1998).

[25] K. Maki, Prog. Theor. Phys. **40**, 193 (1968).

[26] R.S. Thompson, Phys. Rev. B **1**, 327 (1970).

[27] See, for example, V. Ambegaokar, in *Superconductivity*, edited by P. Wallace (Gordon and Breach, New York, 1968), Vol. 1.

[28] P.B. Allen and B. Mitrovic, in *Solid State Physics*, edited by F. Seitz, D. Turnbull, and H. Ehrenreich (Academic Press, New York, 1982), Vol. 37.

[29] J. Keller and V. Korenman, Phys. Rev. B **5**, 4367 (1971).

[30] A.A. Abrikosov, L.P. Gorkov, and I.E. Dzyaloshinski, *Methods of Quantum Field Theory in Statistical Physics* (Prentice-Hall, Englewood Cliffs, NJ, 1963).

[31] V.L. Berezinskii, Zh. Éksp. Teor. Fiz. **61**, 1144 (1971) [Sov. Phys. JETP **34**, 610 (1972)]; J.M. Kosterlitz and D.J. Thouless, J. Phys. C **6**, 1181 (1973); J.M. Kosterlitz, *ibid.* **7**, 1046 (1974).

[32] S. Scheidl and G. Hackenbroich, Europhys. Lett. **20**, 511 (1992); Phys. Rev. B **46**, 14 010 (1992).

[33] B. Horowitz, Phys. Rev. B **47**, 5947 (1993); K.H. Fischer, Physica C **210**, 179 (1993); B. Chattopadhyay and S.R. Shenoy, Phys. Rev. Lett. **72**, 400 (1994); S.R. Shenoy and B. Chattopadhyay, Phys. Rev. B **51**, 9129 (1995).

[34] This crossover to 3D behavior leads to 3D *XY* critical behavior in most high-T_C cuprates [see T. Schneider, Physica B **222**, 374 (1996)], whereas strongly anisotropic materials like $Bi_2Sr_2CaCu_2O_{8-x}$ are more consistent with Bose-Einstein behavior [see, for example, A. Junod, A. Erb, and C. Renner, Physica C **317-318**, 333 (1999); A. Junod, M. Roulin, B. Revaz, and A. Erb, Physica B **280**, 214 (2000)]. However, this point does not affect our results since we work outside of the narrow 3D critical region.

[35] C.T. Rogers, K.E. Myers, J.N. Eckstein, and I. Bozovic, Phys. Rev. Lett. **69**, 160 (1992).

[36] M.J. Ferrari, M. Johnson, F.C. Wellstood, J.J. Kingston, T.J. Shaw, and J. Clarke, J. Low Temp. Phys. **94**, 15 (1994); T.J. Shaw, M.J. Ferrari, L.L. Sohn, D.-H. Lee, M. Tinkham, and J. Clarke, Phys. Rev. Lett. **76**, 2551 (1996).

[37] A.Z. Genack and A.G. Redfield, Phys. Rev. Lett. **31**, 1204 (1973); See also D.E. MacLaughlin, in *Solid State Physics*, edited by F. Seitz, D. Turnbull, and H. Ehrenreich (Academic Press, New York, 1976), Vol. 31, p. 49.

[38] C. Timm, Ph.D. thesis, Universität Hamburg, 1996.

[39] C.P. Slichter, *Principles of Magnetic Resonance*, 3rd ed. (Springer, Berlin, 1989).

[40] S.N. Artemenko and A.N. Kruglov, Phys. Lett. A **143**, 485 (1990); M.V. Feigel'man, V.B. Geshkenbein, and A.I. Larkin, Physica C **167**, 177 (1990); J.R. Clem, Phys. Rev. B **43**, 7837 (1991).

[41] J. Appel, A. Zabel, and C. Timm, J. Low Temp. Phys. **99**, 533 (1995).

[42] C. Timm, Physica C **265**, 31 (1996).

[43] C. Timm, Phys. Rev. B **55**, 3241 (1997).

[44] J. Bardeen and M.J. Stephen, Phys. Rev. **140**, A1197 (1965); see also D.S. Fisher, Phys. Rev. B **22**, 1190 (1980).

[45] R.K. Wangsness and F. Bloch, Phys. Rev. **89**, 728 (1953); A.G. Redfield, IBM J. Res. Dev. **1**, 19 (1957).

[46] H.C. Torrey, Phys. Rev. **92**, 962 (1953).

[47] In Ref. 41 the wrong temperature dependence of n_p is used. The concentration of free vortex-antivortex pairs n_p does not have a jump at T_{BKT}.

[48] M.C. Marchetti and D.R. Nelson, Phys. Rev. B **42**, 9938 (1990).

[49] The diffusion constant D must be sufficiently large so that τ_p is small compared with $1/\omega$ for the magnetic-field fluctuation contribution to be observable; hence $D \sim 10^{-6}$ cm^2/s.

[50] L. Fabrega, J.-M. Triscone, P. Fivat, H. Obara, M. Anderson, M. Decroux, and Ø. Fischer, Physica B **222**, 379 (1996).

[51] J. Kötzler and M. Kaufmann, Phys. Rev. B **56**, 13 734 (1997).

[52] The BKT transition appears to be rather robust against the weak interlayer coupling in Bi-2212 and against disorder; cf. Ref. 51.

[53] A.T. Fiory, A.F. Hebard, P.M. Mankiewich, and R.E. Howard, Phys. Rev. Lett. **61**, 1419 (1988).

[54] The recombination time of a VA pair must be larger than the

typical time scale of the NQR experiment for VA fluctuations to affect the relaxation rates T_1^{-1} and T_2^{-1}. For a similar case—namely, electron spin resonance experiments in semicondutors—the recombination time for an electron-hole pair (10^{-4} s in Si at 300 K) is much larger than the time scale of the ESR experiment (10^{-12}–10^{-11} s).

[55] M.W. Pieper (private communication).

[56] W. Hoffmann, H. Breitzke, M. Baenitz, M. Heinze, K. Lüders, G. Buntkowsky, H.H. Limbach, E.V. Antipov, A.A. Gippius, O. Loebich, H.R. Khan, M. Paranthaman, and J.R. Thompson, Physica C **227**, 225 (1994).

[57] M.W. Pieper, Habilitationsschrift, Universität Hamburg, 1997, p. 26.

[58] R.J. Charles and W.A. Harrison, Phys. Rev. Lett. **11**, 75 (1963).

[59] Let us mention that, in the cuprate superconductors, the ^{63}Cu spin-lattice relaxation time T_1 can be obtained from the spin-echo decay of ^{17}O, which is a measure of the ^{17}O spin-spin relaxation time T_2; cf. R.E. Walstedt and S.-W. Cheong, Phys. Rev. B **51**, 3163 (1995).

[60] S. Wada, J. Phys. Soc. Jpn. **40**, 1263 (1976); C. Berthier, D. Jerome, and P. Moline, J. Phys. C **11**, 797 (1978).

[61] T.F. Smith, R.N. Shelton, and R.E. Schwall, J. Phys. F: Met. Phys. **5**, 1713 (1975).

[62] M.S. Dresselhaus and G. Dresselhaus, Adv. Phys. **30**, 139 (1981).